Reconstruction of the glacier dynamics and Holocene chronology of retreat of Helagsglaciären in Central Sweden

Anna Kurop

Dissertations in Geology at Lund University,
Master's thesis, no 660
(45 hp/ECTS credits)

Department of Geology
Lund University
2023

Reconstruction of the glacier dynamics and Holocene chronology of retreat of Helagsglaciären in Central Sweden

Master's thesis

Anna Kurop

Department of Geology
Lund University
2023

Contents

Cover Picture: View of Helagsglaciären and the extent of the sediments left by the glacier in the Helags valley. Photograph by Anna Kurop, August 2022.

Reconstruction of the glacier dynamics and Holocene chronology of retreat of Helagsglaciären in Central Sweden

ANNA KUROP

Kurop, A., 2023: Reconstruction of the glacier dynamics and Holocene chronology of retreat of Helagsglaciären in Central Sweden. *Dissertations in Geology at Lund University*, No. 660, 34 pp. 45 hp (45 ECTS credits).

Abstract: Despite significant effort put into reconstructing Holocene glacial history in Scandinavia, evidence of glacier fluctuations in Sweden is mostly limited to palaeoclimatic proxies while dating of direct geological evidence from glacier forelands is rare. This is in stark contrast to Norway where the latter is a well-developed practice. The Southern Swedish Scandes in particular have limited research history when it comes to their glaciological and geomorphological record. This study aims to start filling this gap. By using geomorphological mapping, sedimentology, lichenometry and Equilibrium Line Altitude (ELA) reconstruction, I investigate the glacier dynamics, Holocene chronology of fluctuations and palaeoclimatic factors acting on Helagsglaciären, Sweden's southernmost glacier.

Helags valley is occupied by extensive glacial and associated sediments of different ages far beyond the current extent of the glacier, indicating earlier prominent advances dated to 8.5-8.0 ka, around the 9^{th}-10^{th} century AD and around 1789 AD, which was the Little Ice Age (LIA) maximum. Throughout the Holocene, the glacier switched from a polythermal regime with frozen bed at the thinning ice margin and parts of the tongue to a fully temperate one. Today, its southern part remains temperate and active, while the northern became cold-based and is largely inactive. The climate during the 8.5-8.0 ka event was reconstructed to be very cold and wet; slightly warmer and drier during the 9^{th}-10^{th} century AD advance and coldest and driest during the LIA. This agrees well with other paleoclimate and glacier fluctuation reconstructions from Scandinavia and especially Jämtland. It is concluded that small cirque glaciers can uncover a wealth of information about their past dynamics and surrounding climate and thus should be studied more extensively.

Keywords: glacier, geomorphology, lichenometry, sedimentology, palaeoclimate, Helagsglaciären, Holocene

Supervisor(s): Sven Lukas

Subject: Quaternary Geology

Anna Kurop, Department of Geology, Lund University, Sölvegatan 12, SE-223 62 Lund, Sweden.

E-mail: anka212@vp.pl

Rekonstruktion av glaciärens dynamik och holocen kronologi av Helagsglaciären i Mellansverige

ANNA KUROP

Kurop, A., 2023: Rekonstruktion av glaciärens dynamik och holocen kronologi av Helagsglaciären i Mellansverige. *Examensarbeten i geologi vid Lunds universitet*, Nr. 660, 34 sid. 45 hp.

Sammanfattning: Trots att betydande ansträngningar lagts ned på att rekonstruera holocen glacial historia i Skandinavien, är bevis på glaciärfluktuationer i Sverige mestadels begränsade till paleoklimatiska proxies medan datering av direkta geologiska bevis från glaciärens förland är sällsynta. Detta står i skarp kontrast till Norge, där det senare är en väl utvecklad praxis. De södra Skandernas glaciologiska och geomorfologiska historik är i Sverige dåligt studerad. Denna studie har som mål att fylla en del av denna lucka. Genom att använda geomorfologisk kartering, sedimentologi, lichenometri och rekonstruktion av Equilibrium Line Altitude (ELA), undersöker jag glaciärens dynamik, holocena kronologi av fluktuationer samt paleoklimatiska faktorer som verkar på Helagsglaciären, Sveriges sydligaste glaciär.

I Helagsdalen finns omfattande glaciala och tillhörande sediment av olika åldrar, även långt bortom glaciärens nuvarande utbredning. Detta indikerar framträdande tidigare framryckningar daterade till 8,5-8,0 ka, runt 900-talet e.Kr. samt runt 1789 e.Kr. vilket var den lilla istidens maximum. Under hela holocen växlade glaciären från en polytermisk regim med fruset underlag vid den tunna iskanten och delar av tungan till en helt tempererad glaciär. Idag är dess södra del fortfarande tempererad och aktiv, medan den norra delen blev kall och är i stort sett inaktiv. Klimatet under framryckningen 8,5-8,0 ka var enligt rekonstruktionen mycket kallt och blött. Klimatet var något varmare och torrare under 900-talets frammarsch och kallast och torrast under lilla istiden. Detta stämmer väl överens med andra paleoklimat- och glaciärfluktuationsrekonstruktioner från Skandinavien och speciellt Jämtland. Jag drar slutsatsen att små nischglaciärer kan avslöja en mängd information om deras tidigare dynamik och omgivande klimat och därför bör studeras mer omfattande.

Nyckelord: glaciär, geomorfologi, lichenometri, sedimentologi, paleoklimat, Helagsglaciären, holocen

Handledare: Sven Lukas

Ämnesinriktning: Kvartär geologi

Anna Kurop, Geologiska institutionen, Lunds Universitet, Sölvegatan 12, 223 62 Lund, Sverige.

E-post: anka212@vp.pl

1 Introduction

Glaciers are sensitive indicators of climate change and many are reported to have retreated in recent years in response to global warming (IPCC, 2023). Knowledge of the consequences of past glacier retreat can provide us with analogues to the modern situations and be used to predict their future behaviour (Osmaston 2006; Bakke et al., 2010; Lukas and Bradwell, 2010; Gjerde et al., 2016). Reconstructions of the extent and behaviour of palaeoglaciers has thus fuelled our understanding of the current consequences of climate change. In Sweden, considerable effort has been put into constraining the timing and style of retreat of the Scandinavian Ice Sheet (SIS; Svendsen et al., 2004; Krog-Larsen at al., 2009; Krog-Larsen et al., 2012; Stroeven et al., 2016) or mass balance and regime of valley glaciers in the northern provinces such as Sarek and around Kebnekaise (e.g. Karlén, 1988; Kleman and Stroeven, 1997; Carrivick and Brewer, 2004; Radić and Hock, 2006). However, little is known about the chronology and behaviour of cirque glaciers such as Helagsglaciären in the southern part of the Swedish Scandinavian Mountains, despite intensive research on Norwegian glaciers at similar latitudes (Wastegård, 2022). The following review explores the current state of knowledge of the Holocene glaciation history in Scandinavia and, in particular, that area.

1.1 Background: overview of Holocene glaciations in Scandinavia with focus on Jämtland

During the Younger Dryas (12.9-11.7 ka, Rasmussen et al., 2006), Jämtland (and thus Helags valley) was under a thick ice sheet cover (see Figure 1 for the Holocene timeline). Subsequent melting of this ice body uncovered areas surrounding Helagsfjället around 10.4 ka (e.g. Stroeven et al., 2016), marking the start of the local postglacial time. A number of early Holocene glaciations were suggested by Karlén (1988) based on lake sediments in northern Sweden. However, they were questioned by more recent multi-proxy studies (Snowball and Sandgren 1996; Rosqvist et al. 2004). Out of the proposed glaciations, in Jämtland only the 8.5-8.0 ka cooling period appears to be well-documented in lakes (Bergman et al. 2005; Snowball et al., 2002, 2010), a cave deposit (Sundqvist et al., 2007) and a tree-line lowering of 150 m (Öberg and Kullman, 2011) and might correspond to the 8.2 ka 'Finse event' recorded across Norwegian glaciers (Wastegård, 2022). A 1-1.5˚C cooling followed by 2-3˚C warming was suggested for this period in Jämtland (Seppä et al., 2005; Antonson and Seppä, 2007).

The following Holocene Thermal Maximum (HTM, c. 8-5 ka) was very warm in Jämtland, as inferred from maximum tree-line expansion of *Alnus* (Bergman, 2005) around 7.5-7 ka. In northern Sweden, summer temperatures were estimated to be 1.5-2˚C warmer than today (Barnekow 2000). Not much is known about glaciers in Sweden at the time. It is assumed that they were generally absent during the HTM and started growing again only after 6-5 ka as climate gradually cooled down and became wetter due to orbital forcing (Nesje, 2009; Wastegård, 2022).

Shifts to an increasingly wetter and colder climate were reported around 5.8-4.8 ka in Jämtland (Bergman et al., 2005), around 3.5 ka in the Swedish mountains in general (Larsson et al., 2012; Bergman, 2005) and 2.9-2.6 ka in southern Sweden (Digerfeldt, 1988; Andersson and Schoning, 2010). Wide-spread farm abandonment has been documented in Sweden for the latest period (Wastegård 2022), but all three could have contributed to glacier advances.

After a period of relatively dry conditions, a widespread but asynchronous cooling and more humid conditions in Scandinavia occurred between c. 1.7-1.3 ka (Wastegård, 2022). In Jämtland this was noted in lake sediments about 1.8 ka (Andersson et al., 2010), and glaciers in Northern Sweden have advanced around 1.2-1.0 ka (Rosqvist et al., 2004). However, a

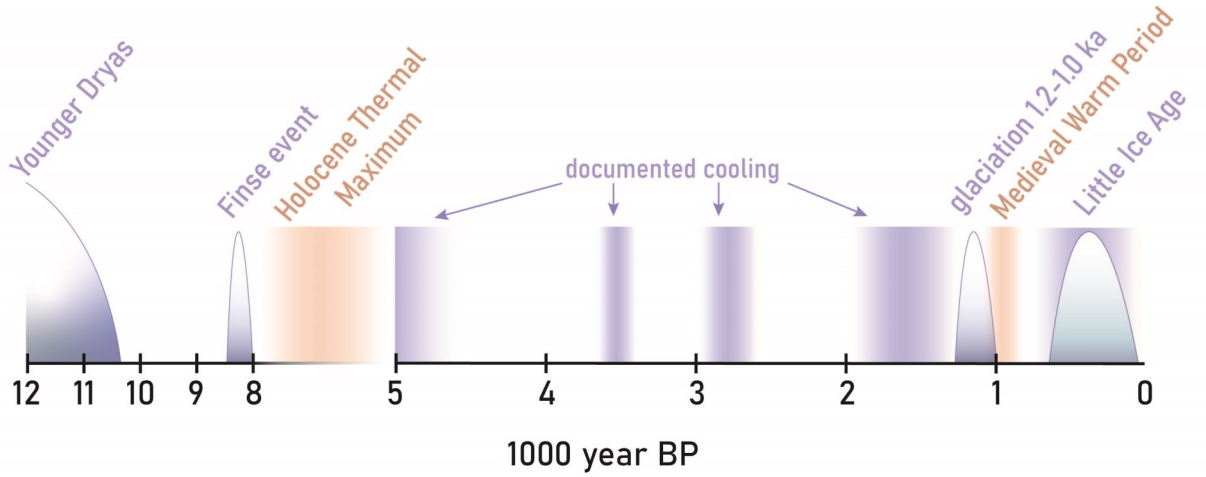

Figure 1. Simplified overview of known climatic changes and glacial advances throughout Holocene in Scandinavia. The timing of events is adjusted to Jämtland. Blue bands mark periods of cooling, orange bands mark periods of warming while rounded 'hills' indicate glacial advances. The severity of each event is not depicted on this figure except for the larger Younger Dryas ice sheet as opposed to subsequent smaller mountain glacerisation.

well-defined Medieval Warm Period (MWP) was inferred from dendrochronological data in Jämtland between 1.1-1.0 ka in the overall trend of cooling over the past 3.6 ky (Linderholm and Gunnarson, 2005).

Following the MWP, the profound cooling known as the Little Ice Age (LIA) has caused glaciers to expand between 1350-1850 AD and it is widely believed that they reached their Holocene maximum positions towards the end of that period (Denton and Karlén, 1973; Karlén, 1988; Nesje et al., 2008).

In the light of the review above, it is clear that evidence of glacier fluctuations in Sweden is mostly limited to palaeoclimatic proxies while dating direct geological evidence from glacier forelands is rare. This is in stark contrast to other Scandinavian countries such as Norway where the latter is common practice (e.g. Matthews, 2005; Bakke et al., 2010; Gjerde et al., 2016). In particular, little work has been done in the southern Swedish Scandinavian Mountains, or the Helags valley itself, compared to elsewhere (see section 2.2 for more details).

1.2 Factors influencing glacier dynamics

Valley and cirque glaciers are topographically constrained ice bodies. The elevation, aspect, and shape of a depression occupied by such glaciers have a profound influence on its behaviour at the ice margin (Kuhn et al., 1985). Apart from the universal factors of climate (in particular temperature and precipitation) that determine the advance/retreat mode of glaciers, their dynamics are also shaped by snowdrift, ice thickness and debris cover (Nesje, 2009). Taken together, that can make topographically confined glaciers rather complex to study.

How a glacier moves is primarily a function of its thermal regime (Benn and Evans, 2010), which is a direct result of the factors mentioned above. Where temperatures reach the pressure-melting point (PMP) at the ice-substrate contact, presence of meltwater facilitates faster ice movement and substrate erosion. On the contrary, temperatures below PMP mean that the glacier sole is frozen to the substrate which limits both ice velocity and its erosive power. Thermally, glaciers can be classified as warm-based (temperature > PMP), cold-based (temperature < PMP) or polythermal and they can switch between these states on seasonal or longer timescales. These changes have a significant impact on the kind of sediments they leave behind and any given glacier's sensitivity to climate change (Glasser and Hambrey, 2001).

In line with the paucity of studies on glaciers in the Scandes, little is known about the thermal regime of small glaciers such as Helagsglaciären (Holmlund and Jansson, 2003).

1.3 Aims

This study aims to contribute to the reconstructions of Holocene history of glaciers in

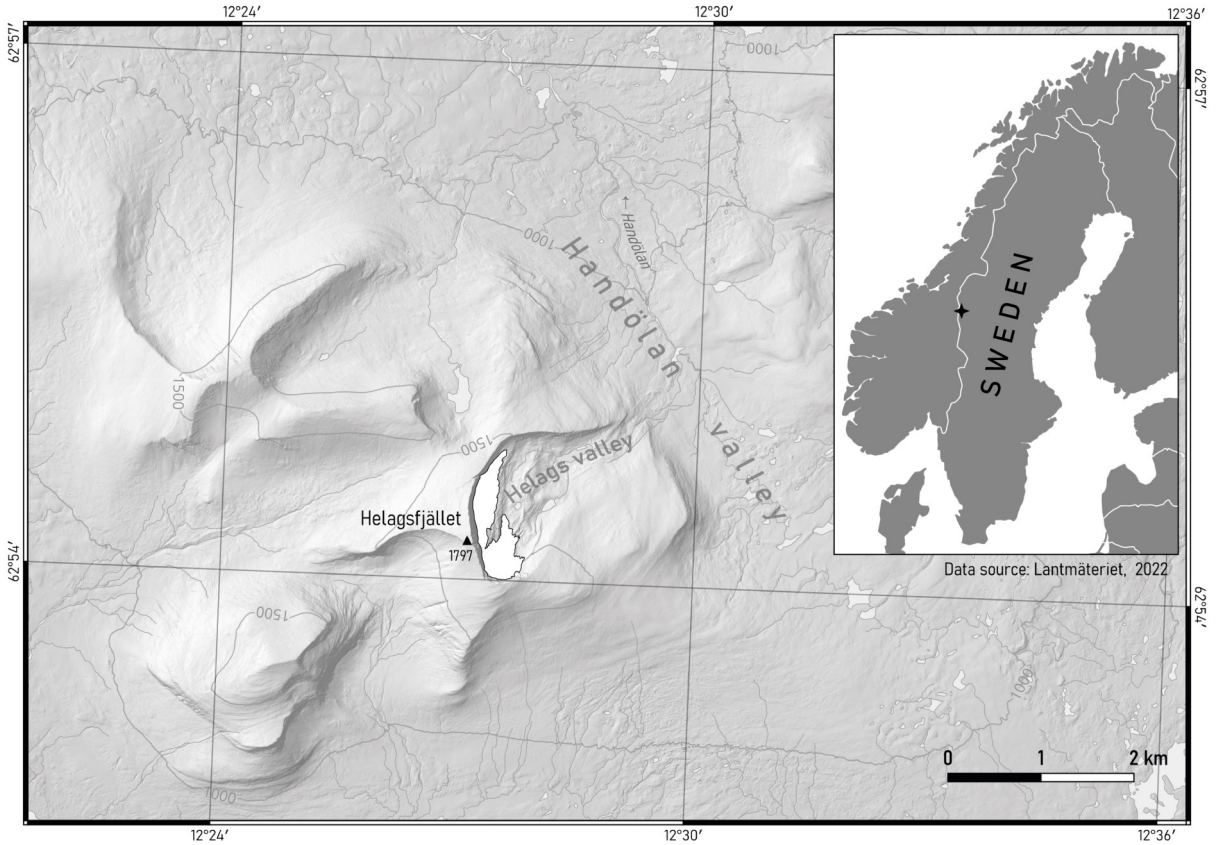

Figure 2. Location and topographical setting of Helagsglaciären. The glacier occupies a cirque cut in the eastern side of Helagsfjället, which is the highest peak of a mountain massif built from resistant paragneiss. The cirque and its extension Helags valley drain to Handölan river valley that run to the north-east.

Scandinavia by looking at Helagsglaciären, Sweden's southernmost glacier. By combining geomorphological mapping, sedimentology, lichenometry and palaeoclimatic proxies, it seeks to establish the times when the glacier advanced and retreated, its dynamics and thermal regime at these times, as well as to assess whether these conditions have changed through time. This study also seeks to elucidate the relationship between the glacier's behaviour and governing climatic factors. In doing so, it would be able to answer the broader question on the significance of small cirque glaciers in reconstructing palaeoclimate.

2. Site description

2.1 Geological and climatic setting

Helagsglaciären is located in the southern Swedish Scandinavian Mountains (Figure 2). It occupies a 1.5 km wide cirque the floor of which lies at 1420-1320 m above sea level (a.s.l.) and is cut into the eastern side of Helagsfjället (1797 m a.s.l.). The Helags valley drains into Handölan river valley. The mountain is built from resistant paragneiss with some amphibolite, formed ca. 542-488 Myr (SGU, 2017). It stands out among relatively wide and flat terrain from which other individual flat-topped peaks emerge. The area is situated well above the local tree line (around 850 m a.s.l.). Mean summer (Jun-Aug) and winter (Dec-Feb) temperatures are about 8 and -6°C respectively, and precipitation equals 1300 mm, mostly as rain in the summer season (SMHI, 2013). The moisture is mainly brought from the North Atlantic by the westerlies. However, there is a precipitation gradient across the Scandinavian Mountains due to orographic effects and increasing continentality. Despite closeness to the North Atlantic coast, most of the moisture is scavenged by the Norwegian part of mountains to the west.

2.2 Previous research on Helagsglaciären

To the author's knowledge, to date only limited research has been conducted on Helagsglaciären and its deposits. The earliest known study is the general descriptive work of Enqvist (1910) in which he focused on the elevation of the glacier ice and its margins, measurements of the firnline as well as basic geomorphology of moraines on the glacier's direct foreland. The study was supplied with photographs of Helagsglaciären and its surroundings and a couple of general topographic maps. Enqvist (1910) speculated about the former greater extent of the glacier based on flat-topped, 'wind-eroded' ridges up to 2 km downvalley of the ice margin at the time, but without any definite statements. The first identification of the lowermost moraine (1042 m a.s.l.) on the floor of Handölan valley as the maximum extent of Helagsglaciären was made by Bergström (1955). He also attempted to assign age of deposition to landforms in the Helags valley. The outermost moraine in the valley was referred to as 'lateglacial'. Additionally, deposition around 500 and 1750 AD was suggested for two upvalley endmoraine complexes in large distance from each other, though the exact location is unclear.

Lundqvist (1969) mapped the Helags valley using an aerial photograph taken on the 5th Aug 1960. This publication was a description to Jämtland's Quaternary sediment types map created by SGU, but it also included and reviewed information on local mountains and glaciers. From the photograph, Lundqvist (1969) identified the main latero-frontal moraine ridges from the cirque's headwall to about half the valley's length. That study also noted a considerable retreat of the ice margin since the report by Enqvist (1910).

More recently, Helags valley was mapped as a part of SGU Quaternary geomorphology maps at general level of detail, with some landform identification (Figure 3). Kullman and Kjällgren (2000) report a radiocarbon date on a fossil pine stump extracted from a little mire in the Helags valley to be

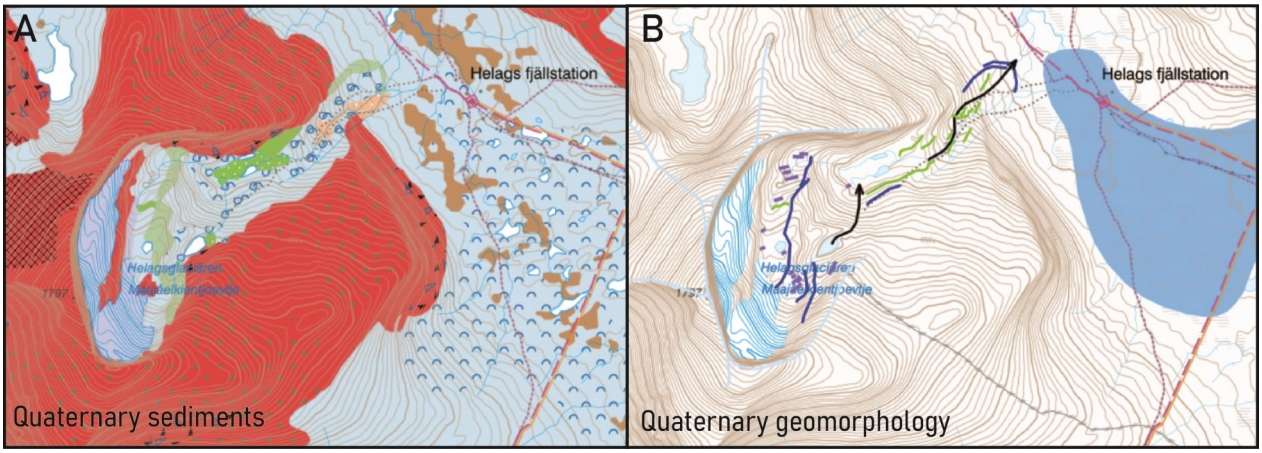

Figure 3. Geological Survey of Sweden's (SGU) current maps depicting Helags valley and its sediments. A – Quaternary sediments (sw. Jordarter; SGU, 2021) and B – Quaternary geomorphology (sw. Kvartär geomorfologi; Blomdin et al., 2021). The reader is referred to the original publications for explanation of the legend.

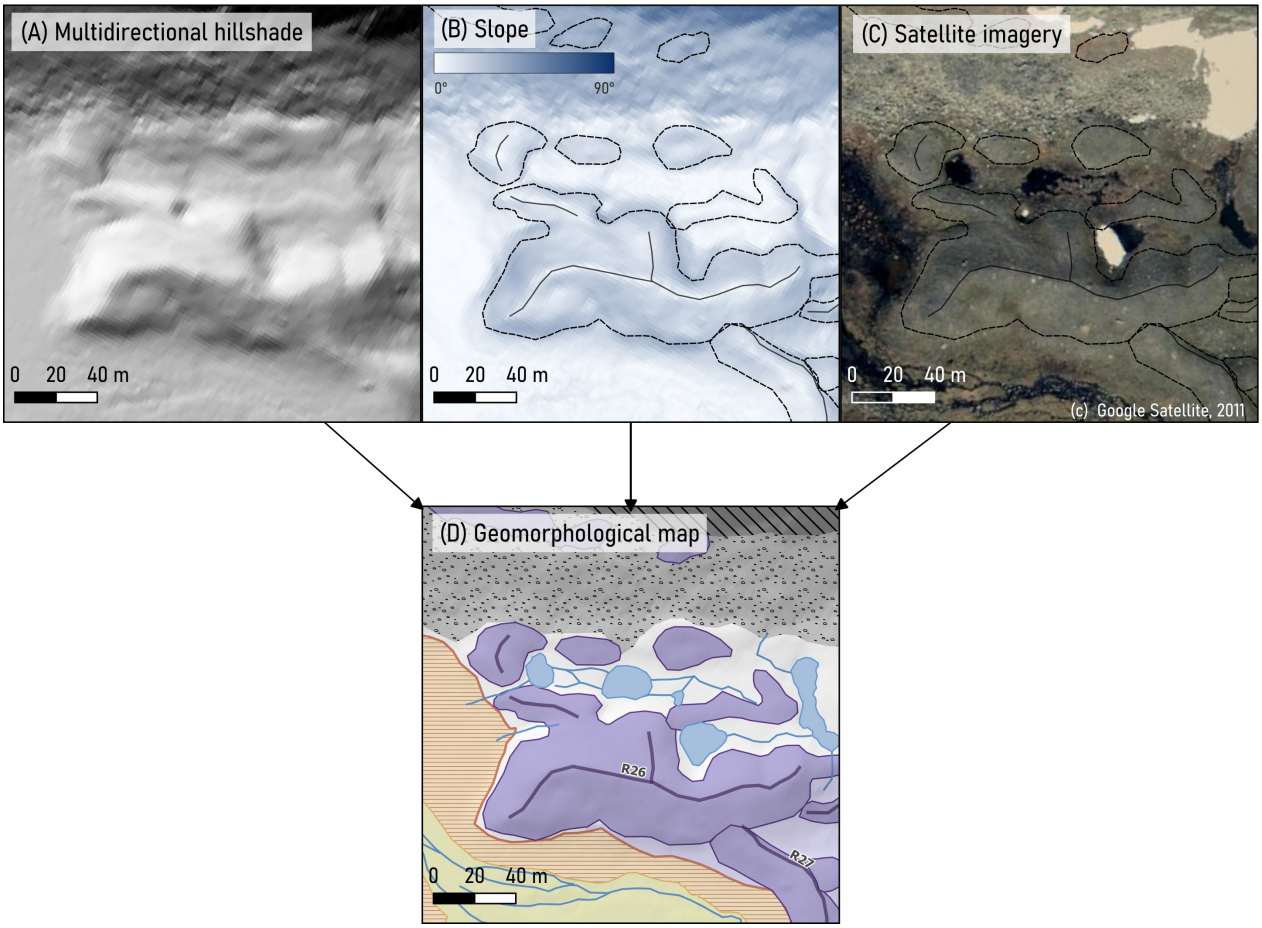

Figure 4. Remote digitising of geomorphological landforms using (A) a multidirectional hillshade, (B) a slope layer and a (C) Google Satellite image from 2011, which was the most recent summer image of the area. The selection of the final map (D) is the result of synthesising remotely-sensed and field data.

11 160 ± 80 yr BP (recalculated using IntCal 20 [Reimer et al., 2020] to 11 170 cal yr BP with 11 237 and 10 939 cal yr BP as upper and lower limit, respectively). Lastly, Helagsglaciären was mentioned by Ericsson Rehn (2019) as a glacier that 'should not exist' due to negative mass balance but survives thanks to protective cirque topography, snowblow and north-east orientation.

3. Methods

The methodology of this study falls into three consecutive stages: remote, field and data post-processing methods. However, for integrity each method is described here as a self-contained process, while the workflow during the mapping includes all three stages.

3.1 Geomorphological mapping

The mapping followed guidelines by Chandler et al. (2018), where remote assessment and introductory mapping of the terrain is first carried out before validation in the field. For this purpose, LiDAR-based Digital Terrain Model (DTM) sheets with 1.0 ± 0.3 m and 1.0 ± 0.1 m horizontal and vertical resolution, respectively, were downloaded from Lantmäteriet (2022) and examined using QGIS 3.28 software. The very high resolution was necessary to catch small features produced by a single valley glacier. The landform shapes (e.g. ridges, flat plains, channels) were preliminarily outlined as polygons (if more regular) or vector lines (if long and narrow) and digitised in QGIS with a focus on detailed delineation of terminal and lateral moraines. Due to large scale of the final map, no size selection was necessary as it was possible to include most mapped features. For clear visualisation of the terrain, a multidirectional hillshade function was used where illumination from four light sources is combined (azimuths 225˚, 260˚, 315˚, 360˚; angle 45˚) to extract both high- and low-relief features. This technique bypasses overlooking some parts of relief due to excessive shading or overexposure to light that is common in traditional single-directional hillshade models, and it has been widely applied in various forms to mapping glacial landforms (e.g. Hughes et al., 2010; Norris et al., 2017). A slope function was also used to aid feature recognition by marking breaks of slope as outlines and crestlines of

moraines, and a satellite image provided by Google (Figure 4).

Field work was carried out from 3-13th August 2022, during which the preliminary geomorphological mapping was validated and refined by field mapping. Large-scale features were first observed from a high vantage point before proceeding to systematically walk the terrain in quasi-straight lines where possible (Chandler et al., 2018). Particular effort was put into outlining shapes and marking crests of moraine ridges using the QField mobile application geolocation and tracking functions (OPENGIS.ch, 2022). All newly recorded information was drawn digitally in QField and later exported to QGIS for the creation of the final map. The map design is based on the Swedish Geological Survey (SGU) cartographic standard (SGU, 2021) with modifications to suit the context of the study.

3.2 Sedimentology

The exposures were dug by hand and examined using standard approaches. At the end of the examination, they were refilled back with sediment. Once the outcrop surface had been cleaned of debris, the largest features were logged first and later filled in with detail (Evans and Benn, 2021). Due to relatively small sizes of the outcrops, a tape measure was used to establish the true 2D proportions of each exposure. Lithofacies analysis was carried out on-site and included description of grain size, lithology, sorting, roundness, colour, structural features and nature of contacts of different lithofacies. Two-dimensional logs were created on paper using Krüger and Kjær's (1999) recommendations for graphical key for displaying different features.

The logs were then scanned and digitised in Adobe Illustrator 2022, and Krüger and Kjær's (1999) key was modified to suit the context of the study.

3.3 Lichenometry

Lichenometry was first proposed as a relative dating technique by Faegri (1934) and developed by Beschel in the 1950s (eg. 1955, 1957, 1958). The theory behind lichenometry is based on the fact that lichen are long-lived pioneers that start to occupy rock surfaces soon after they stabilise at the Earth's surface. If the growth rate of a lichen is known, the time of the surface exposure can be calculated (see reviews by Bradwell and Armstrong, 2007; Benedict, 2009; and examples of case studies by Evans et al., 1999; Winkler, 2004 and Leigh et al., 2020). However, the growth rate depends on many local factors such as temperature, humidity, slope aspect or rock type and thus is unique to the site. It also varies by lichen species. This facilitates the need to create a lichen diameter-age calibration model by measuring lichen on surfaces of known age before applying lichenometry to a specific area.

Rhizocarpon geographicum in particular has been utilised in most studies as it is widespread in polar and alpine environments (Armstrong, 2016). However, the *Rhizocarpon* genus comprises many similar-looking species that make *R. geographicum* particularly difficult to identify without years of expertise. For this reason researchers tend to use the name '*R. geographicum'* as an umbrella term for this plus all other lichen species that can be mistaken for it, most notably *R. alpicola* (Innes, 1983; Evans et al., 1999; Armstrong, 2016), and therefore admit the risk of misidentification. Despite the uncertainty this introduces (each species has a different growth rate), the approach still yielded satisfactory results (O'Neal, 2006). This practise is also adopted here.

Out of many approaches to measure lichen diameters, the one proposed by Evans et al. (1999) was

Figure 5. Measuring the longest lichen diameters using a calliper (left) and a plastic ruler (right). Photographs by O. Zheleznyy

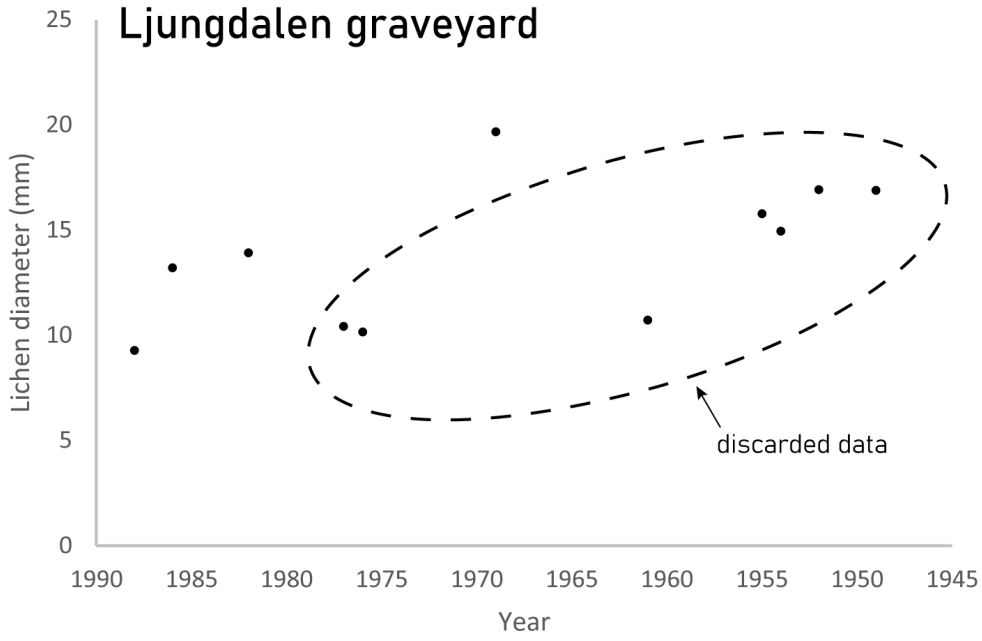

Figure 6. Lichenometric data from the graveyard in Ljungdalen. The points in the dashed circle represent disrupted growth of lichen

chosen for this study as it is quick, efficient and relies on basic assumptions of lichenometry while attempting to eliminate some biases related to anomalous lichen. It was also shown to be a reliable and accurate method (Bradwell, 2009). In principle, the mean of diameters of the five biggest thalli of *R. geographicum* found on boulders building a moraine ridge is used to infer its age. Any thallus ≥20% bigger than the next in a dataset is removed as an outlier.

The selected boulders had uniform lithology (gneiss) and were located on the distal slope of a ridge to avoid the cooling effect of catabatic winds from Helagsglaciären. That was also done to ensure that boulders that once crowned the crest but toppled over with time are also sampled as they were likely to host the oldest lichen. A calliper with 0.1 mm precision was used to measure the lichen, especially in the initial stage when measuring specimens for the age-diameter calibration curve. This was later changed to a simple plastic ruler with precision of 1 mm when measuring diameters larger than 10 cm as the calliper was simply too short for this task (Figure 5).

A multitude of sources was used in order to construct the calibration curve. The nearest cemetery in Ljungdalen (62°51'17.3"N 12°46'27.3"E; 18 km south-east from Helags valley) was investigated for old graves erected using local stone (paragneiss or granite), and 11 tombstones were sampled, the oldest having been erected in 1949. Out of them only four were used as it became apparent that the others had been disturbed (e.g. cleaned) after preliminary age-lichen diameter plotting (Figure 6). An older cemetery in Storsjö (28 km from Helags) was also visited, but without satisfying results as most graves were made of concrete or metal.

The last source used for constructing the calibration curve was the website Svenska glaciärer – an inventory of Swedish glaciers lead by Per Holmlund (Bolin Centre for Climate Research, 2017). From there, photographs of Helagsglaciären taken in 1895, 1908, 1930 and a scanned map published in 1969 were downloaded (Figure 7 and references in the caption). From these, moraine ridges at which the ice margin was located in the respective years were identified and sampled for lichen diameters. This resulted in a small dataset of independent age control on those particular moraines. A similar approach of using independent age control has recently been used in the European Alps (Carturan et al., 2014).

3.4 Equilibrium Line Altitude calculation

Once the ice margins had been drawn at six different time steps that were established based on the lichen-derived chronology (1960, 1930, 1890, 1790, ~700 and ~100 AD), the approximate glacier surface elevation contours were drawn in QGIS 3.28 at 10 m interval for each time step, and then converted to a Digital Elevation Model (DEM) with 1 m resolution using SAGA GIS 7.8.2. The DEMs were then used to calculate the Equilibrium Line Altitude (ELA) at each time step using the Area-Altitude Balance Ratio (AABR) method by Osmaston (2005), using a script written in Python (see Appendix).

The balance ratio (BR) reflects the ratio of slopes of net mass balance-altitude curves above and below the ELA (Figure 8). There are three important assumptions underlying the AABR method: the gradients are linear, the ratio remains fixed in time and the glacier is well constrained by topography. Rea (2009) gives a good overview of reasons these assumptions are feasible and hold true for many glaciers. He also calculated the 'typical' BRs for different kinds of glaciers across the world using the World Glacier Monitoring Service (WGMS) mass balance data. Out of this dataset, three AABRs are suitable for Helagsglaciären and thus are used in this study to calculate ELAs: the global AABR of 1.75 ± 0.71, mid-latitude maritime AABR of 1.9 ± 0.81 and Western Norway AABR of 1.5 ± 0.4 (Rea, 2009).

The transfer function to infer palaeotemperature

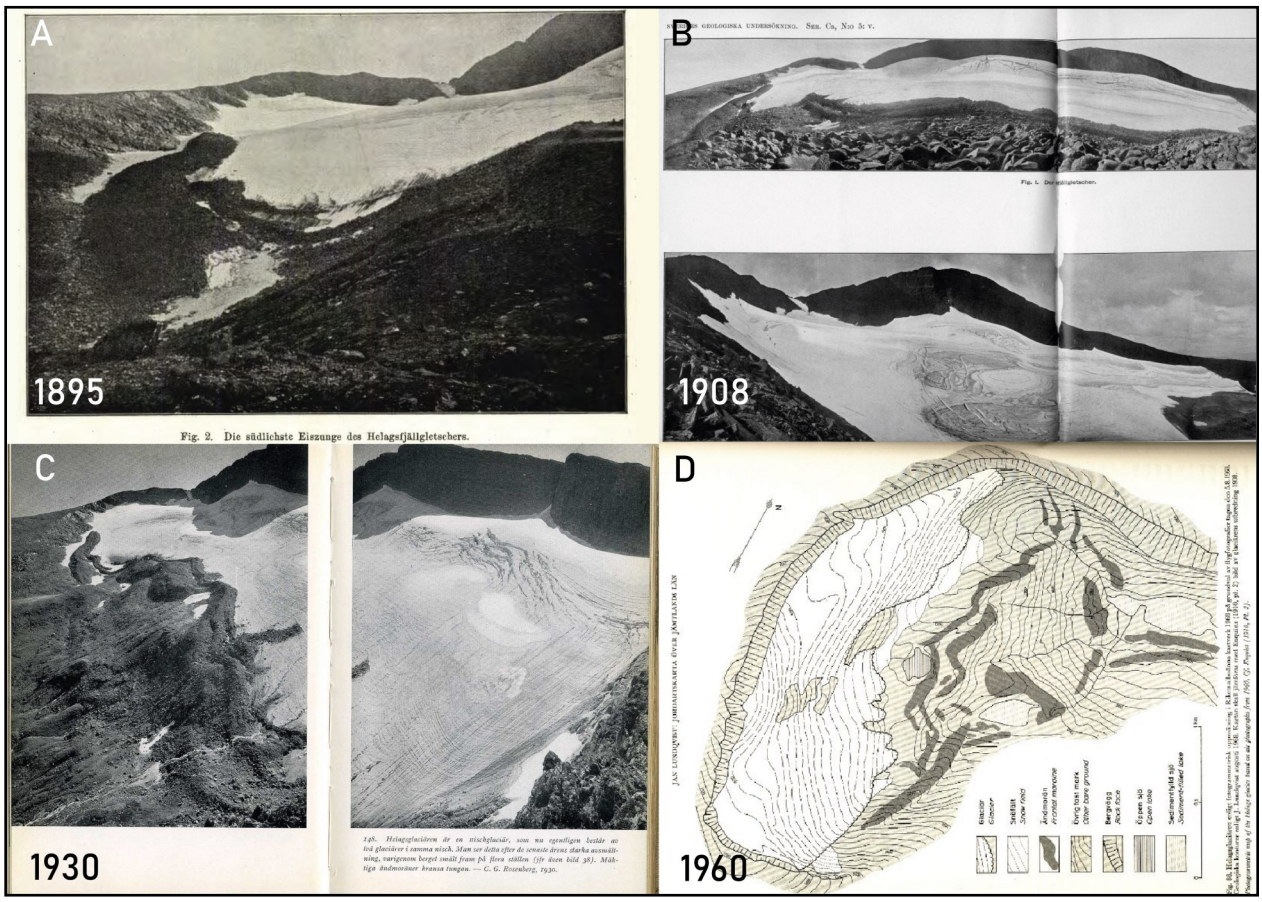

Figure 7. Old photographs used to identify moraines of certain ages for calibration of the age-lichen diameter curve. References: A, B – Enqvist (1910); C – Fries (1931) ; D – Lundqvist (1969).

and precipitation at an ELA was taken from Ohmura et al. (1992) who used mass balance data from 70 glaciers distributed globally to derive it. As such, it is not ideal as the relationship between the summer temperature and annual precipitation depends on continentality of climate (Carr et al., 2010). However, there are no such relationships derived locally and thus the global dataset is the best available option to avoid circular reasoning (Benn and Ballantyne, 2005; Lukas and Bradwell, 2010; Boston et al., 2015; Chandler and Lukas, 2017). The equation

$$P_a = 645 + 296T_3 + 9T_3$$

represents the annual precipitation (P_a) at the ELA as a function of mean summer temperature (T_3 – June, July, August).

The mean summer temperature was taken from Zhang et al. (2016) who reconstructed temperature using tree rings in Jämtland at altitude 650 m a.s.l. Their record spans 1160 years. The earlier Holocene temperature value was taken from Velle et al. (2005) who derived it from chironomids in five different lakes in Scandinavia, one of them being in Sylarna 20 km north of Helags valley. The temperature and precipitation values were adjusted to the ELA for the calculation, and sea level for later comparison using the mean air temperature lapse rate of 0.6˚C/100 m and 8%/100 m (after Haakensen, 1989).

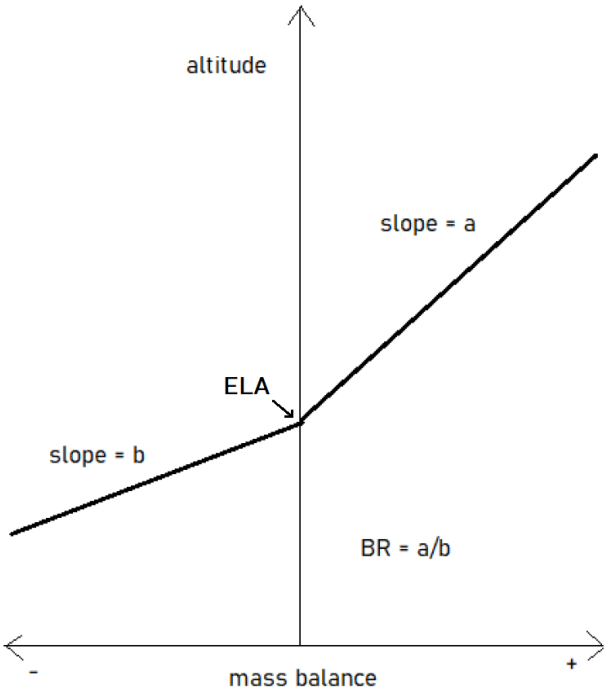

Figure 8. Balance ratio (BR) as a ratio of slopes of mass balance curves against altitude of a glacier. An ELA is where mass balance = 0.

4. Results and interpretation

4.1 Geomorphological mapping

The final geomorphological map is presented in Figure 9. Helagsglaciären occupies an asymmetrical, ~2 km long valley with an impressive 1.5 km wide cirque accommodating two almost-separate ice masses: a southern one lying in a possibly overdeepened niche and a northern one resting on a long, narrow (~300 m) bedrock shelf. The southern ice unit extends into the glacially moulded and occasionally streamlined bedrock basin whose elevation descends from the south to the north. The northern part is more overdeepened than the southern one. Some striae were noted with bearing parallel to streamlining (Figure 10). The bedrock basin is covered with a thin veneer of moraine debris and boulders which becomes scarcer towards the northern end. The outlet edge of the bedrock basin is topped by an extensive system of multi-crested, partly lobate moraine ridges built with subangular and angular boulders, out of which two main sets can be distinguished (R11 and R12-14, Figure 11 A and B). The southernmost fragment of this system (R6) is flattened, diffuse and appears to have flutes with an azimuth of about 045˚ on its surface in contrast to two crescent ridges below it (R10 and below). The southern part of the basin is flanked by a prominent lateral moraine (R9) whose crest elevation is descending down-valley and also seems to consist of two parts, the lower one bordered by a set of smaller ridges (Figure 11C). Below, a field of large angular boulders occupies the area before one enters a basin infilled with lacustrine and fluvial sediment. This is in turn bordered by a large, broad and weathered lobate-shaped moraine (R15-17) that separates it from a long steep step (with an average slope of 35˚) that dissects the Helags valley into two parts. Extensive talus debris accumulates on the southern wall of the cirque.

The step between the upper and lower parts of Helags valley descends about 140 m and comprises heavily dissected and reworked diamictic sediment with individual hummocks occasionally standing out (Figure 11A). Numerous active and periodic meltwater channels cut through this undulating surface. The step terminates on a large but discontinuous asymmetric moraine ridge in which the first sediment outcrop was dug (R23, outcrop 1). The ridge has a long distal but very short proximal slope adjacent to a waterlogged flat basin.

The floor of the lower level of Helags valley, below the threshold described above, is at 1230 m a.s.l. and is mostly occupied by extensive lacustrine sediments partially reworked by streams, a lake nested within them and two sets of lateral moraines running alongside it, parallel to the valley walls (Figure 12A). The crestline of the outer lateral moraine (R24) follows the 1260 m contour while the inner one's (R25) runs subparallel around 1250 m a.s.l. The southern set is much better preserved than the northern one, which was either eroded or covered by talus. Solifluction lobes are well developed on the sides of Helagsfjället outside the range of the lateral moraines (Figure 12C). A couple of channels run along the distal slopes of the southern set of moraines, occasionally cutting through them. The outer lateral moraine becomes progressively more fragmented down-valley. The large lake plain is enclosed on its downvalley side by a low quasi-arcuate ridge with a gentle proximal slope and steep distal one (R27). The ridge is cut by the stream draining the lake plain and much of it is thus eroded. In the north-east section of this level there is an area of seemingly unordered low-amplitude hummocks and periodically water-filled depressions, some linked with blindly-ending small streams. The area is restrained by a larger, bran-

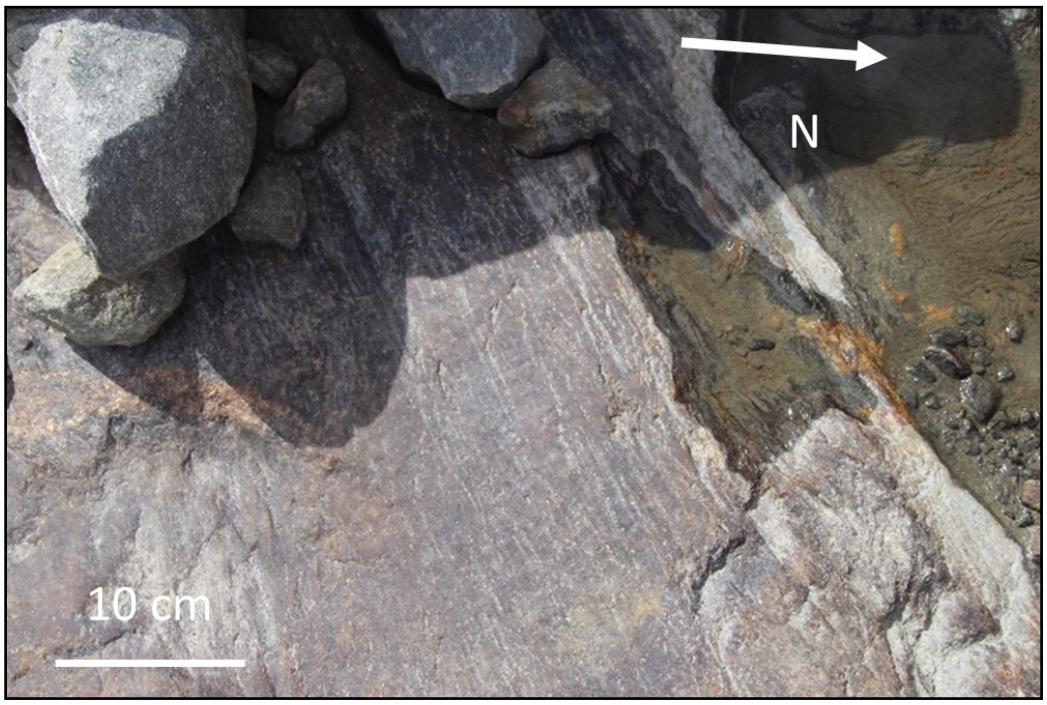

Figure 10. Striae on the surface of exposed bedrock in the Helags cirque.

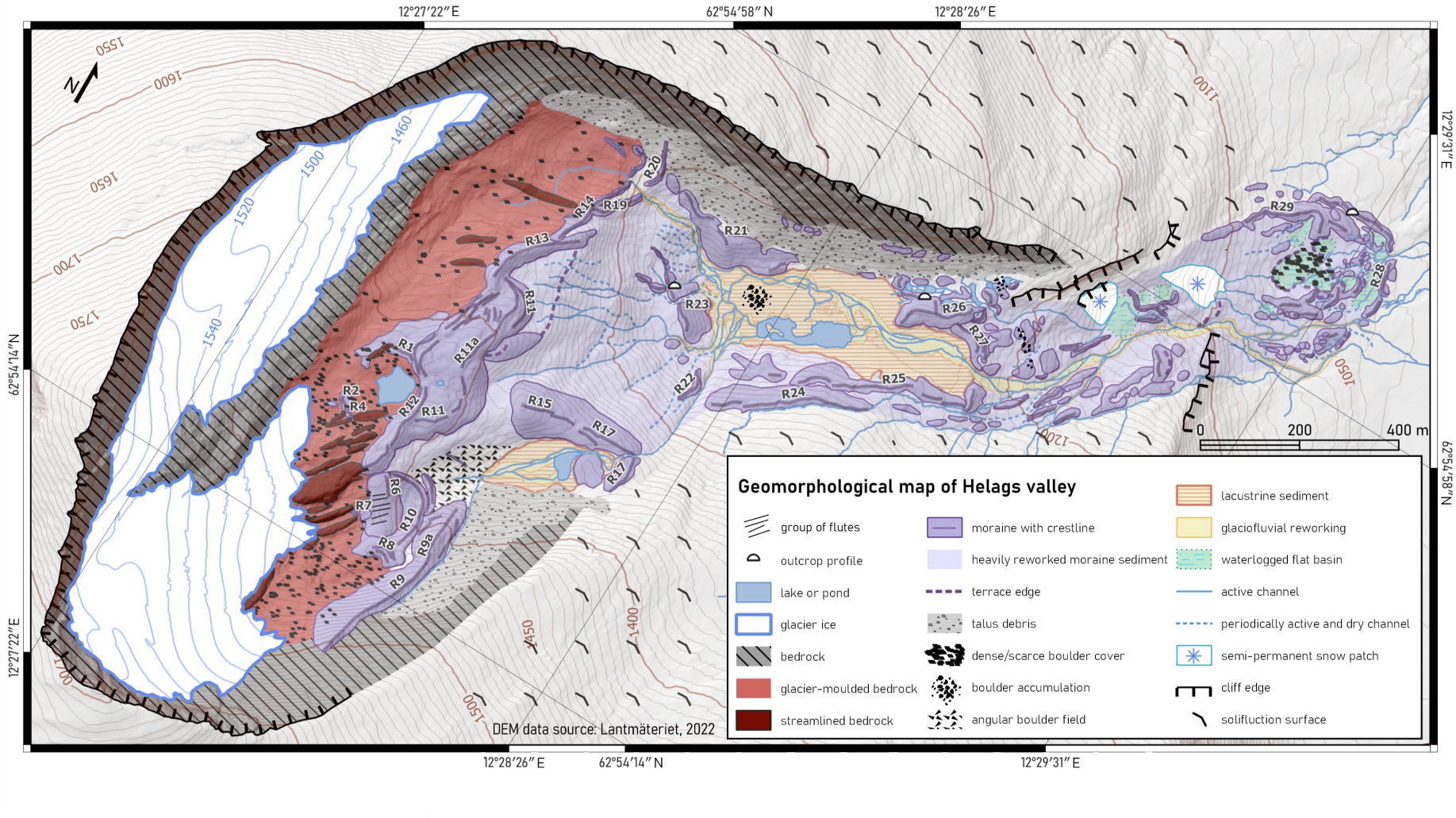

Figure 9. Geomorphological map of the Helags valley. The valley can be divided into two parts: the cirque or upper part where the current glacier is located and the lower part with a large lake plain bordered by two lateral moraines from the southern side. The maximum range of Helagsglaciären's sediments extends to the Handölan valley floor where they form a set of two arcuate moraine ridges. The names R1-R28 refer to moraine ridges sampled for lichenometric dating.

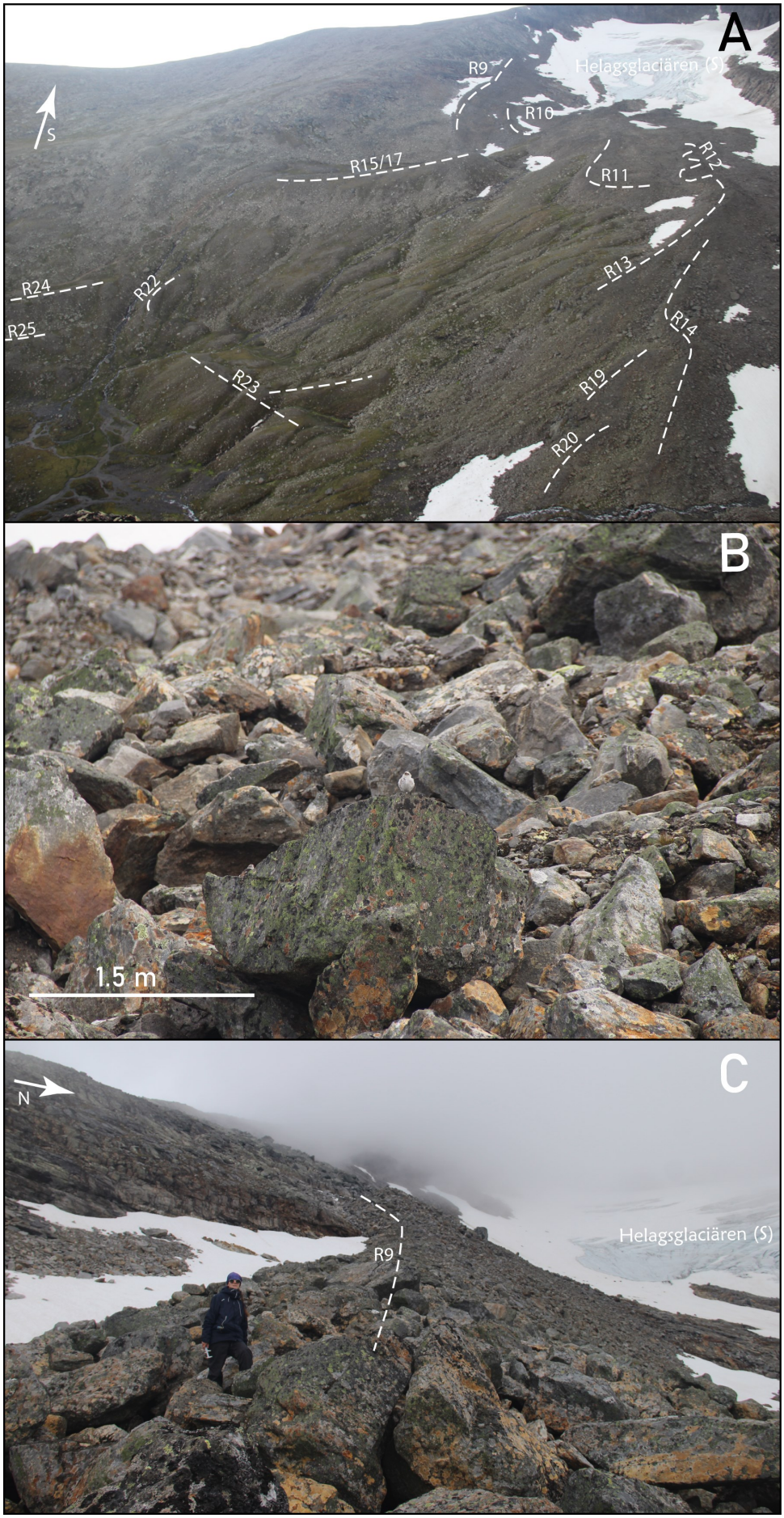

Figure 11. Helagsglaciären's foreland. Crestlines of landforms marked on Figure 8 and dated with lichenometry are traced with dashed lines. A – multi-crested moraine at the edge of the Helags cirque (R10-20), reworked sediments below it and a fragmented ridge at the upvalley end of the main lake plain (R23). The smaller lake plain is behind R15/17. B – angular boulders building most of the sediments in the upper part of the Helags valley. C – example of the surface of a moraine ridge from the upper reaches of the valley. Photographs by O. Zheleznyy.

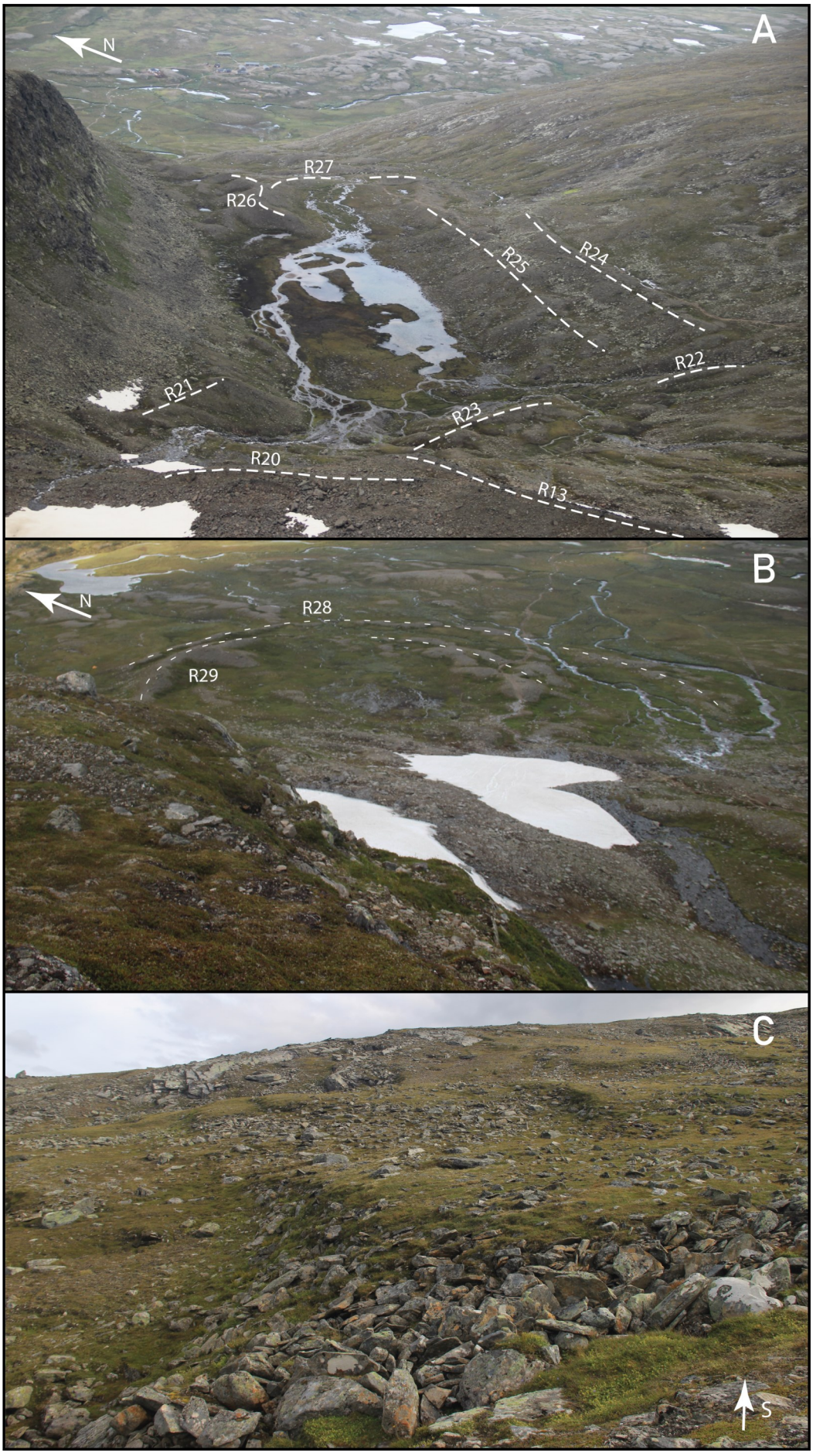

Figure 12. A – lower part of the Helags valley largely occupied by the main lake plain dammed by R27 and a set of two lateral moraines (R24-25). B - Handölan valley. A set of two arcuate ridges (R28-29) marking the outermost limit of sediments deposited by Helagsglaciären. C – solifluction lobes outside the range of glacial sediments in the Helags valley.

ching elongated ridge (R26) that separates it from the lake plain. Outcrop 2 was dug on R26's northern side. The area extends into a rocky shelf and is partly covered by talus.

The area extending downvalley from the lake plain is characterised by its steeper slope and common reworking and fragmentation of moraines by multiple streams. Most notably, the southern side of the main stream channel is occupied by elongated ridges that are subparallel to the main valley axis while the northern side accommodates mostly irregular, transverse or rarely subparallel ones, with multiple dry depressions between them. In the lower northern part of this sector there are two semi-permanent snow patches. The upper one sits in a deep niche underneath a rock cliff with waterlogged flat terrain in front of it while the lower one rests on a debris-covered slope of Helagsfjället.

Following a rocky cliff that develops into a gentler slope northwards, the sediments expand about 400 m beyond the Helags valley onto the floor of Handölan valley (Figure 12B). The sediments form two sets of clear arcuate moraine ridges. The outermost moraine (R28) is of lower height (10 m) and dissected into individual linear ridges and hummocks by streams draining the Helags valley. It has an undulating crestline and occasional little dry channels incised into its outer slopes perpendicularly to the crestline. Outcrop 3 was dug on the northern proximal slope of R28. The inner arcuate ridge is of higher height (R29, up to 20 m) and located at a 0-30 m distance from the outer one, with channels running between them. The inner set is characterised by multiple crestlines, some of them bifurcating, dry/waterlogged depressions and occasional fragmentation into hummocks by streams draining the interior of the lobe. The interior of the ridge itself comprises a series of semi-circular waterlogged basins with clear terrace edges on the upglacier side, from which streams emerge. The entire interior area is covered in scattered boulders that range from 0.5 to 2 m in their a-axes lengths.

4.2 Sedimentology

Three outcrops were dug and logged in three different moraine ridges in the lower parts of the Helags valley (see Figure 8). The sediments in the upper parts of the valley contained too many boulders to enable any logging.

4.2.1 Outcrop 1

This outcrop (Figure 13) was dug by excavating

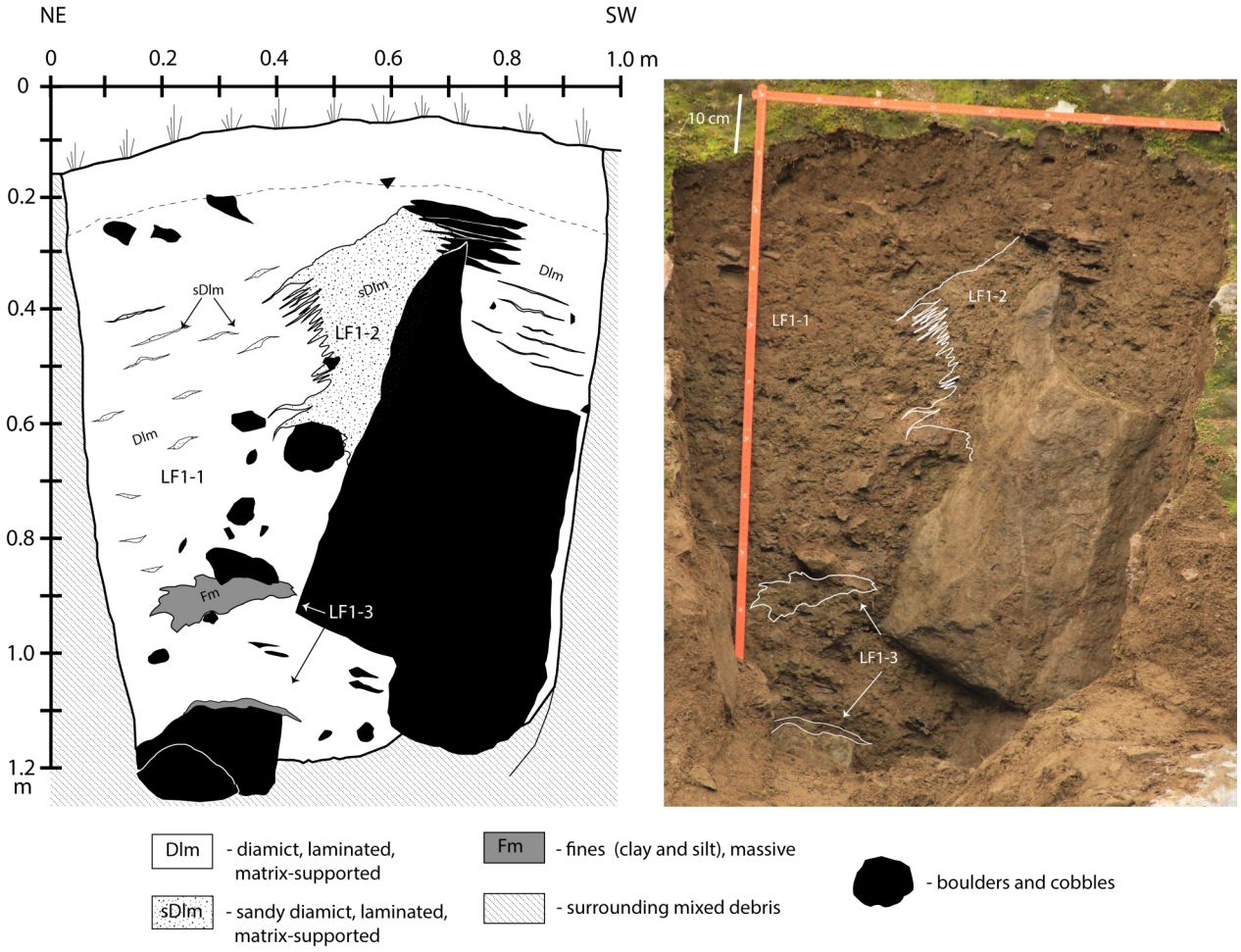

Figure 13. Sedimentological log of outcrop 1 dug in R23 (Fig. 9 for location). LF refers to different lithofacies, as in the main text.

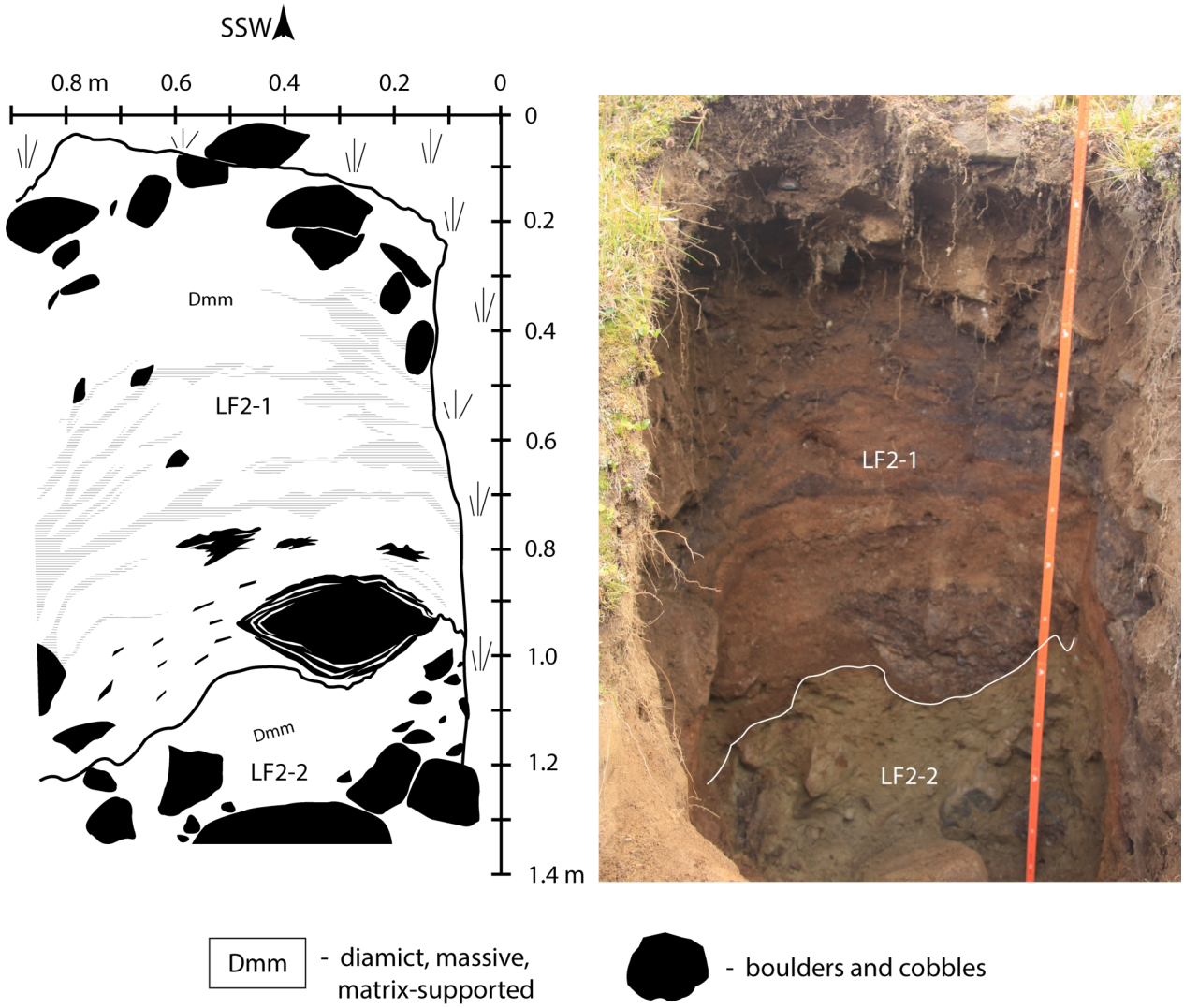

Figure 14. Sedimentological log of outcrop 2 dug in R26 (Fig. 9 for location).

a wall of a channel incision in landform R23. The resulting exposure is small (1x1.2 m) and shows an irregular arrangement of boulders in a finely laminated, weakly consolidated and matrix-supported diamict (LF1-1). The sense of lamination is given by long and narrow streaks of sandy sediment in the upper, northern part of the outcrop gently dipping NE, which gradually become more of poorly-sorted sandy pockets in the lower parts of it. Nearly half of the exposure is occupied by a large sub-angular boulder with a protruding 'horn' on which a weathered clast is lodged. The sandy streaks dip gently towards SW on its southern side. On the northern side of the boulder the diamict becomes much more sandy and extends outwards, interfingering with the less sandy matrix (LF1-2). A few clasts are draped in this zone. A notable feature is a warped, elongated massive clay inclusion (LF1-3) on which a cobble is resting. A lens consisting of similar clay sediment is resting on a surface of another large boulder in the lower part of the section.

4.2.2 Outcrop 2

This outcrop (Figure 14) was dug in the north-facing slope of landform R26 and has also a small size (1x1.4 m). There are two distinctive lithofacies there separated by a sharp undulating contact. The upper one (LF2-1) is a poorly sorted and weakly consolidated diamict of a rusty colour. In the upper part of it there is a concentration of subangular boulders which are completely absent from the middle and only reappear again near the contact, often as heavily weathered and easily crumbling clasts. Numerous blackish flame-like wisps are interspersed throughout this lithofacies. LF2-1 attains a more intense rusty colour in the ~5cm directly above the contact.

The lower lithofacies (LF2-2) is a massive matrix supported sandy clayey diamict that is much better consolidated than the upper one. It has a light brownish-grey colour and hosts subangular to subrounded interlocking boulders that increase in numbers downwards so that it was impossible to dig further than 1.4 m.

4.2.3 Outcrop 3

This outcrop (Figure 15) consist of three parts roughly at right angles to each other and was dug in the proximal side of the northern fragment of ridge R28. The transect was dug 1.4 m into the landform until the crest was reached, and so Figure 14 presents the frontal view (segment I) and two wings (segments II and III) of the resulting blind trench. The end moraine consists of three lithofacies resting on each other. LF3-1 is up to 30 cm thick and made of darkening up, rust-coloured sandy clayey silt that generally represents the soil and vegetation influence. LF3-2 is a weakly consolidated gravelly silty sand that in segment III shows a faint lamination dipping downslope. There is a more sandy pocket within it interfingering with LF3-2 in segment II. A sharp undulating contact separates LF3-2 and LF3-3. LF3-3 consists of interlocking subangular and subrounded boulders with a sandy, angular gravel matrix between them. The entire sediment is very weakly consolidated and readily disintegrates at the slightest touch. The arrangement of boulders seems chaotic when viewed in segment I, though the long axes of many of them point downwards. When viewed in a profile (segments II and III), the boulders' long axes are arranged sub-parallel to the slope and give an impression of downslope alignment. Such weak stratification is also visible in the gravels of the matrix between the boulders that in some places even form distinct pavements resting on the top surface of a boulder (e.g. boulder D). Some boulders look bullet-shaped (e.g. F, E and G).

4.3 Integrated interpretation of the processes involved in the dynamics of Helagsglaciären

4.3.1 The Handölan valley

The outermost moraine (R28) is interpreted as having been built by loose debris flows (LF3-3) dumped from the ice margin during stable conditions, consisting of supraglacial (the angular gravel fraction) and subglacial (rounded boulders and bullet-shaped clasts) material. This interpretation is based on the mixed, unsorted clasts giving a chaotic impression but revealing a semi-arranged pattern indicative of flow downslope. A notable absence of deformation structures indicate that the material was deposited through passive release (dumping) and not disturbed by the ice margin anymore (by e.g. pushing), similarly to the process described by Krüger et al. (2002). The roundness of boulders and especially their bullet shapes indicate that active transport processes were present probably throughout the length of the glacier, which suggests warm-based conditions at most of the glacier's sole (Kleman et al., 1997). LF3-2 represents better-sorted and finer-grained sediment deposited on the moraine irregularly along the ice margin (varying thickness) by glaciofluvial processes. Occasional sand lenses might be evidence of lower-velocity channels on the surface of this dump moraine. The silty, dark soil layer capping the moraine (LF3-1) indicates that a long time has passed since the deposition of R28. The uneven, undulating crestline of R28 might point to the existence former ice cores, suggesting a frozen ice margin. The southern fragment of R28 displays a number of little dry channels incised into its slopes perpendicular to the crestline which might be a trace of meltwater runoff routes.

Several insights can be also gained from the pattern of crestline bifurcation of moraine ridges. In the Handölan valley, R29 upvalley from R28 is simply a smaller version of R28, indicating an approximately uniform decrease in volume of the glacier's tongue (both along its front and sides). However, this moraine exhibits three crestline bifurcations which suggest an active retreat and a snout sensitive to changes in mass balance (Boston and Lukas, 2019). That would furtherly translate to a possibly wet-based glacier that was closely coupled to climate during this phase of overall retreat.

4.3.2 Lower part of the valley

Areas of frozen ground

The two sets of prominent lateral moraines (R24-25) reach up to 40 m in height, suggesting a thick ice body occupying the valley at the time of its maximum extent. They are bordered by impressive meltwater channels cut at their distal sides in the adjacent non-glacial sediments. According to Benn and Evans (2010), such distinct incisions are characteristic of a glacier margin frozen to the ground so that the meltwater cannot penetrate below it. It is typical for many cold-based glaciers where permafrost is common (Kleman et al, 1997; Greenwood et al, 2007), though it has also been documented at temperate glaciers (Syverson and Mickelson, 2009). The solifluction lobes observed on the Helags valley slopes directly adjacent to the lateral moraines, but never on them, could also point to the fact that at the time of the moraine deposition, Helagsglaciären was cold-based at least at its margins. This is because presence of permafrost enhances the solifluction processes and indicates a much colder climate. However, the lobes may also have formed before moraine formation and thus, remain being unequivocal.

Reinardy et al. (2019) have shown that temperate glaciers can contain areas of frozen bed where ice thickness is less than 10 m or where permanent snow rests on the surface of a glacier. These circumstances would result in englacial thrusting at the snout or development of hummocky controlled moraine at stagnant ice zones. A similar process is suspected to have happened in the area north-east of the large lake plain where outcrop 2 was dug. The undulating contact between LF2-1 and LF2-2, diamictic chaotic sediment with many boulders of LF2-2 and hummocky (in descriptive terms) geomorphology with multiple small circular basins and blind channels suggest that this is a dead-ice meltout area. Similar structures have been reported from known dead-ice landforms (e.g. Evans and Benn, 2021: Fig. G.27). Comparable topography inside the range of R28-29 moraines implies that some

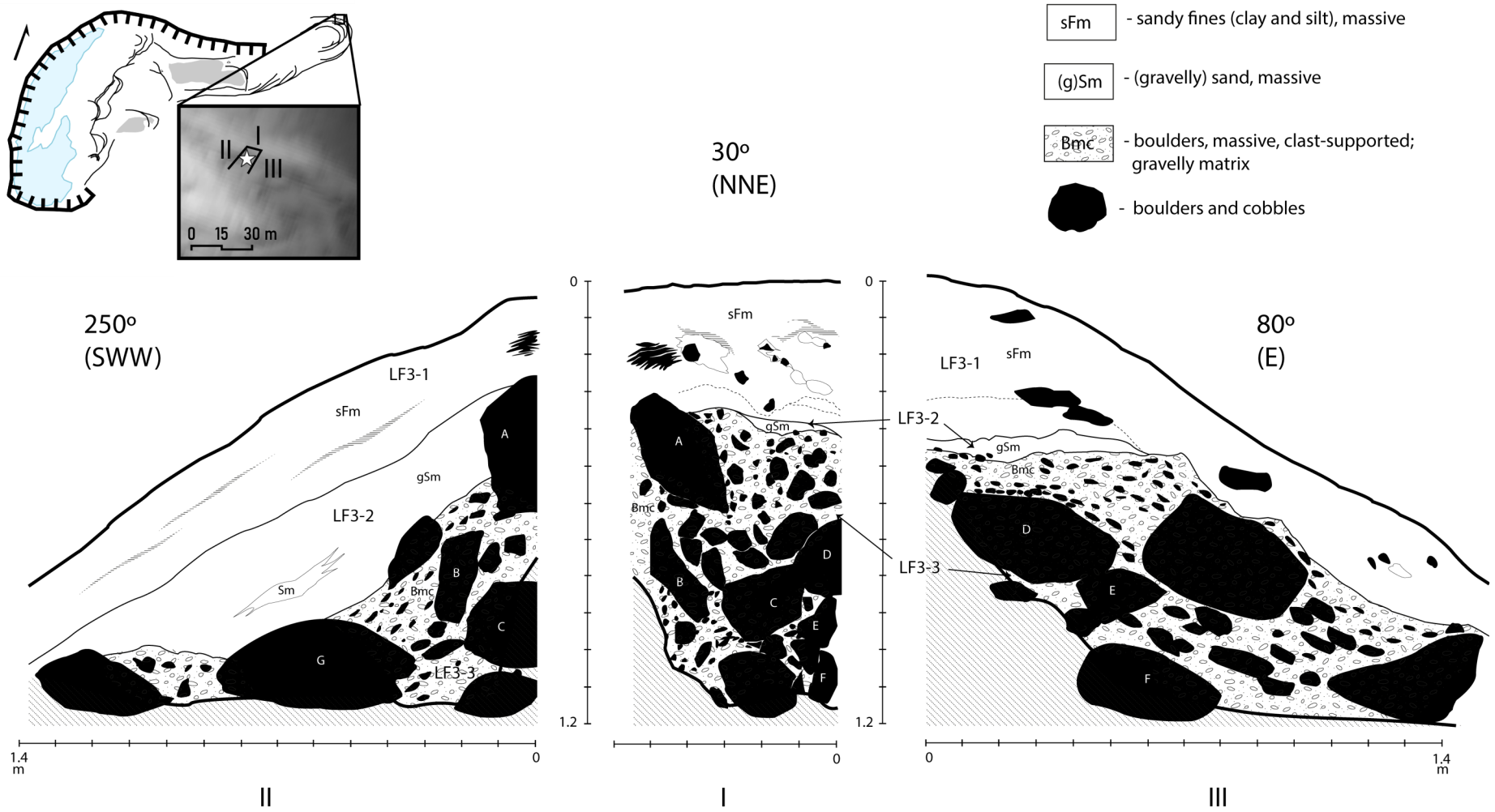

Figure 15. Sedimentological log of outcrop 3 dug in R28. Frontal view (section I) and two wings (sections II and III) of a trench dug into the proximal side of the moraine ridge. Boulders are lettered for clarity of description and identification, e.g. boulder A in section I and II is the same boulder viewed from different angles; boulders E, F and G exhibit bullet-shaped morphology (as in main text).

dead ice blocks might have detached there as well (cf. Kjær and Krüger, 2001; Lukas, 2011).

Areas of active retreat

The western end of the larger plain contains a set of landforms suggestive of a single-front oscillatory ice margin indicative of a temperate glacier. Most notably, the bifurcating crestline of R23 and the neighbouring parts of lateral moraines (R21 and R25) as well as a set of channels running parallel to them indicate active retreat, similarly to the evidence discussed by e.g. Boston and Lukas (2019). This is furtherly supported by the laminated nature of LF1-1 in outcrop 1, the draping of clasts and a warped stoss-lee shaped clay inclusion which suggests that some degree of deformation was involved in building R23. Therefore, the boulder accumulation zone present at the lake plain near R23 is interpreted as boulders dumped off the ice margin, in line with observations from modern ice margins (Wyshnytzky et al. 2021; Rettig et al., 2023). The proglacial lake was probably too shallow for the glacier to reach its floatation point and thus to support a calving margin, but it cannot be ruled out that individual dropstones might be scattered throughout the plain.

The moraines in the lower part of Helags valley contain fine matrix which indicates involvement of subglacial transport before sediment deposition during earlier glacier advances. However, most of the sediments between the cirque and R23 have been heavily reworked by meltwaters from the retreating glacier and gravitational processes so that little can be deduced from them now. Helagsglaciären seems to have been divide into two individual flow units around that site. The southern flow unit of Helagsglaciären produced a proglacial lake dammed by R17 that was drained through breaching. That resulted in a deeply incised channel running below it that flows into the larger lake plain dammed by R27.

4.3.3 Upper part of the valley

The upper part of the valley exhibits plenty of erosional forms (such as streamlined bedrock or striae) typical for debris-rich basal ice that is also warm-based because regelation (melting and freezing) must have happened to incorporate boulders into it (Benn and Evans, 2010). The streamlined bedrock forms indicate the movement direction out of the valley. The different bearing of these forms in the northern and southern part of the cirque indicate that there are two rather independent lobes of Helagsglaciären. Striae noted on the surface of the bedrock point to basal sliding that would only be possible if liquid water was present (Lipovsky et al., 2019), suggesting that temperatures at the sole of the glacier reached the PMP in the upper part of the valley.

The sinuous moraine ridges at the rim of the

Figure 16. Current ice margin of the southern part of Helagsglaciären. A mixture of predominantly angular debris of different sizes melts out from debris bands and is dumped on exposed bedrock. Boulders are also embedded in the lower parts of the glacier. Pebbles frozen to the glacier sole were observed inside the cavity in the centre of the image.

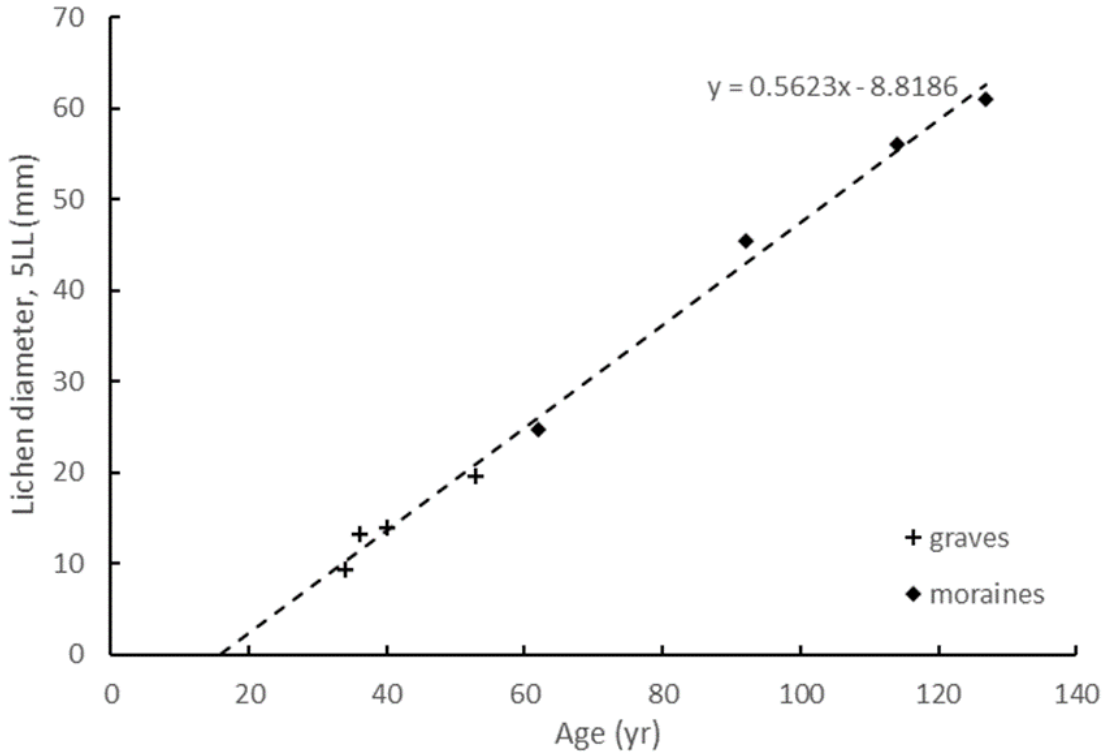

Figure 17. Lichen diameter-age calibration curve for Helagsglaciären's foreland. 5LL stands for the mean of the five largest lichens.

cirque (R12-13) reflect an unfocused and gradually retreating ice front with several stillstands when conditions changed. The cirque's width is probably responsible for the very close spacing between individual crestlines as the glacier's response to mass balance changes was distributed across a wider ice front compared to the more enclosed lower part of the valley. The angular and subangular boulders building this moraine suggest a predominant supraglacial debris transport route.

Several crestline bifurcations are found along the rim moraine R6-R20. They imply three distinct ice bodies forming lobes or glaciologically distinct flow units earlier in time (southern, middle and northern flow units marked by R10, R11 and R20 respectively). All of them seem to have been active despite a significant size reduction of Helagsglaciären compared to its maximum limit. The three individual flow units probably only start acting as one when they coalesce as the ice gets funnelled towards the narrower lower part of the valley during times of sustained positive mass balance.

Observations of subrounded pebbles frozen to the sole of the southern part of the glacier suggest that the glacier is still actively eroding the substrate despite its significant size reduction in recent years. The current ice margin contains a mixture of material from large angular boulders embedded in ice or resting on top of it, to finer angular debris melting out from the ice surface in distinct bands (Figure 16). As such, the currently deposited sediments probably reflect input from all three transport routes – supraglacial, englacial and subglacial.

4.4 Lichenometry

The complete calibration curve is presented in Figure 17. It is based on eight calibration points and covers 127 years.

In order to extend the timeline even further, I reviewed other lichenometric calibration curves from research sites across Norway and Sweden, and found the best fit with the Eastern Jotunheimen curve from Matthews (2005). This dataset extends to about 250 years back in time and is based on historical measurements, photographs, maps and assumed ages of certain landforms due to several other lines of evidence pointing to it. The formula of the curve was modified by subtracting 20 from it to better fit calibration data in this study. The final form of the equation is:

$$\log(y + 130) = 2.1916594 + 0.00353252x$$

where y is surface age and x is lichen diameter in mm. When tested on the calibration set, this equation resulted in calculated ages only 1-3 years different from the true independently-calibrated ages at Helags valley. This modified equation was then used to calculate the ages of all the sampled moraine ridges in the Helags valley that were outside the calibration dataset obtained locally.

The calculated ages and corresponding years for different landforms in the Helags valley are presented in Table 1. They range from 52 years for moraines closest to Helagsglaciären to over 2000 years for the southern lateral moraines. The general trend yields increa-

Table 1. Calculated ages of landforms in the Helags valley. JotE refers to ages calculated using the modified Eastern Jotunheimen curve of Matthews (2005). 'True age' is based on the moraine identification in the photographs from Figure 7.

ID	Lichen diameter (5LL, mm)	Age (yr) JotE	Year AD (JotE)	Error	True age
R4	19.66	52	1970	20	
R5	24.74	60	1962	20	1960
R6	45.4	95	1927	20	1930
R6	44.1	93	1929	20	1930
R7	8.36	36	1986	20	
R8	41.94	89	1933	20	
R8 (gully)	59.04	121	1901	20	
R9	71.72	149	1873	20	
R9a	103.04	229	1793	20	
R10	60.94	125	1897	20	1895
R11	104.26	233	1789	20	
R11a	85.44	182	1840	20	
R12	56.12	115	1907	20	1908
R13	85.74	182	1840	20	
R14	72.56	151	1871	20	
R15	224.4	835	1187	200	
R17	268.2	1247	775	200	
R20	84.32	179	1843	20	
R21	253.4	1091	931	200	
R23	201.8	673	1349	200	
R24	330.2	2151	-129	200	
R25	333.0	2203	-181	200	
R26	221.0	808	1214	200	
R28	315.8	1899	123	200	

sing ages with distance from the glacier. However, a few exceptions to this start to appear in the lower level of the Helags valley and the Handölan valley (e.g. R23, R25, R26). The ages agree very well with the moraines used for calibration (R5, R6, R10 and R12), instilling confidence in the results from the upper part of the Helags valley. The furthest and oldest moraine ridge from that part (R11) yields an age of 233 years, which corresponds to year 1789 (R11), about 100 years older than the oldest calibration point.

The credibility of the data decreases significantly for the sediments in the lower part of the Helags valley due to the lack of calibration points, increased fragmentation and reworking of landforms, and increased difficulty in finding suitable lichen to measure that have not demonstrably coalesced. This is manifested in age reversals (e.g. the inner lateral moraine R25 yields an older age than the outer one R24; R26 is younger than sediments upvalley) and age inconsistency of data points from the same landform (e.g. the outermost R28 and outer lateral moraine R24 both mark the same limit but R28 is younger than R24 according to the lichen data if taken at face value). The lichen in the lower part of the valley were commonly irregularly shaped or were found to have coalesced with others. While such individuals were avoided, there is a risk that the suture zone between two lichen was unrecognisable and thus a pair (or group) of lichen was sampled as one. This would give highly erroneous ages, a risk that increases with age (Bradwell, 2010).

Another point of caution is the reworking of sediments that would topple over and bury boulders from the crest of a ridge and expose new boulder surfaces for lichen colonisation. This is a common source of error on latero-frontal moraines (Humlum, 1978; Lukas et al., 2012). This process is suspected on R23 and R21 as the former lies at the foot of a steep slope with multiple streams fragmenting it and thus the age of 673 years (deposited in 1349) as at best an estimate of the boulder exposure age but not deposition. The latter lies under a steep cliff, is reworked and partly buried.

Due to the uncertainties tied to the measurements in the lower part of the valley, the resultant numerical ages from there are discarded and landforms R21-28 are from now referred to as simply *early Holocene in age*.

A special case is made for R15-17 which refer to two parts of the same lobate structure delineating the smaller lake plain at its north-eastern end. Due to their different morphology they are likely to represent two different events which is supported by resultant years of deposition in around 1187 (R15) and 775 AD (R17) and spatial arrangement (the older one is further from the glacier snout). However, large uncertainty is placed on them because of the age limit of the method and lack of calibration points in the immediate vicinity.

4.5 Equilibrium Line Altitude calculation

The ELAs for respective time periods and glacier types are presented in Table 2. Within the error limit, they show a rising trend from about 1370 m a.s.l. during the early Holocene advance to about 1510-1500 m a.s.l. in the 20th century. The ELA was only about 20 m lower during the local LIA maximum than at present. The values differ by up to 17 m between the glacier types (as in Rea, 2009), but the difference is more typically less than 10 m. The lowest ELAs are for marine temperate type while the highest – for the Norwegian-type glaciers. The 1930, 1960 and 2014 values were calculated due to the availability of data about the ice margin position at those times. However, Helagsglaciären was then experiencing a rapid thinning and retreat and thus was not in equilibrium. Therefore, these values should be treated with great caution as long-term averages of the glacier's mass balance conditions in the 20th and 21st century.

Table 3 shows the calculated temperature and precipitation values for selected time periods corresponding to maximum limits of glacial advances (early

Table 2. Calculated ELAs from Helags valley, using the AABR method of Osmaston (2005) and accumulation-ablation balance ratios of three different glacier types after Rea (2009).

	ELA (m a.s.l.)													
year AD	early Holocene	±	775	±	1790	±	1895	±	1930	±	1960	±	2014	±
Glacier type:														
global	1375	36	1468	19	1492	16	1501	14	1488	15	1501	13	1511	11
marine temperate	1369	39	1465	20	1490	16	1498	16	1486	16	1499	14	1509	12
Norwegian	1386	21	1474	11	1497	9	1505	11	1492	9	1505	8	1514	7

Holocene, c. 8-12th century, c. 1789 AD and c. 1900 AD) or glacier hypsometry data available from 20th century (1930s and 1960s), adjusted to the sea level. The temperature oscillated within a 1˚C-difference. The lowest values are for 1789 AD and the earlier Holocene advance. The latter, however, has a precipitation value at the ELA that is 250 mm higher than at present while the period around year 1789 seems to be the driest out of all. The 8th–12th centuries advance was nearly equally cold but 120 mm wetter than the 1789 one. The last LIA advance – around 1900 AD – was almost as cold as in the 8-12th centuries but slightly wetter. The 20th century experienced gradually warmer and wetter conditions.

Table 3. Temperature from Zhang et al. (2016) and Velle et al. (2005) adjusted to the ELA using 0.6˚C/100 m temperature lapse rate (T at ELA); and calculated precipitation at the ELA (global glacier type; P at ELA). Both are adjusted to the sea level for comparison (last two columns) using the temperature lapse rate mentioned above and precipitation lapse rate of 8%/100 m (after Haakensen, 1989).

Period	ELA (m)	T at ELA (˚C)	P at ELA (mm)	T at sea level (˚C)	P at sea level (mm)
early Holocene	1375	2.65	1493	10.90	711
900s	1468	2.25	1356	11.05	623
1790s	1492	1.94	1252	10.89	571
1900s	1501	2.09	1304	11.10	592
1930s	1488	2.98	1606	11.91	733
1960s	1501	2.99	1610	11.99	732

5. Discussion

5.1 Changing dynamics of a small valley glacier

Throughout the Holocene, Helagsglaciären experienced a lot of changes in its mass balance due to changing climate. As a result, its dynamics and geomorphological imprint on the landscape also changed. However the glacier's thermal regime appears to have remained remarkably consistent for most of the Holocene, likely because of its small size and location at the lower latitude in the Scandes. During periods of larger extents, the evidence suggests that Helagsglaciären was a polythermal glacier with an active and climatically-sensitive snout that was only frozen to the ground near the margins where ice was thin, similar to the glaciers currently found in high Arctic areas (Irvine-Fynn et al., 2011) or southern Norway (Reinardy et al., 2019). Once the ice retreated to position R23, the climate was warm enough to prevent widespread permafrost formation and the funnelled ice was likely thick enough for PMP to be reached throughout. The glacier exhibited an entirely temperate regime up until the 20th century when it got gradually fragmented into first three, then two independent flow units, one of which is currently stagnating and probably cold-based and the other is actively flowing, but may soon follow this pattern due to rapid thinning. A change in ice thickness has been identified as a major factor determining a change in thermal regime in many contemporary glaciers throughout the Arctic (Mooers, 1990; Reinardy et al., 2013, 2019; Tonkin et al., 2016; Mallinson et al., 2019).

A large influence on the dynamics of Helagsglaciären is the glacier's hypsometry and valley topography. Funnelling of ice once it exits the cirque makes the ice margin particularly sensitive to changes of the mass balance when it reaches the narrower lower part of the valley, resulting in widely spaced moraine ridges. In the upper level the response to climatic changes result in only a slight retreat/advance due to much wider ice front. Similar conclusions were reached by Kuhn et al. (1985) in the study of Alpine glaciers. The factor of topography should be carefully taken into account when interpreting a valley/cirque glacier's behaviour from its moraine sequences.

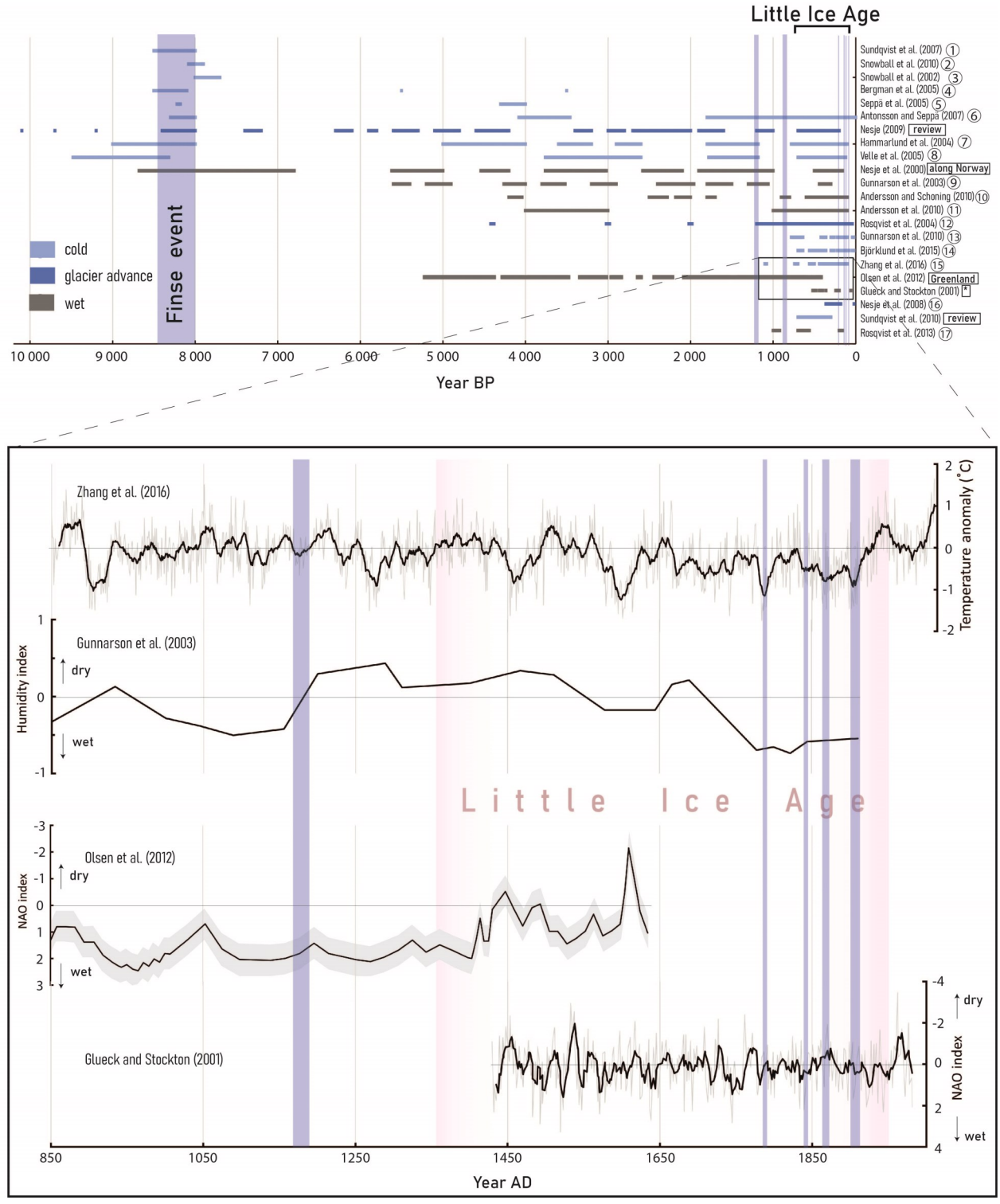

Figure 18. Compilation of proxy temperature and precipitation reconstructions and inferred times of glacial advances. Blue bars represent inferred times of expanded Helagsglaciären. An accompanying map (the next page) shows numbered location(s) of the reviewed studies. In frame: a zoom-in onto the last 1150 years where more detailed records are available. The black line in Zhang et al. (2016) and Glueck and Stockton (2001) is a 10-year running mean. The grey band in Olsen et al. (2012) is uncertainty.

5.2 Chronology, its strengths and limits

The chronology for sediments in the Helags valley derived from lichenometry is not complete due to the dating limit of the method. However, several important points can be deduced from it.

The Helags valley represents sediments from glaciations far earlier than the LIA, which is in agreement with Bergstrom (1955) and Lundqvist (1969) and disagrees with the widely-held consensus that glaciers in Scandinavia reached their Holocene maxima during the LIA (Karlén, 1973; Nesje, 2009). For Helagsgla-

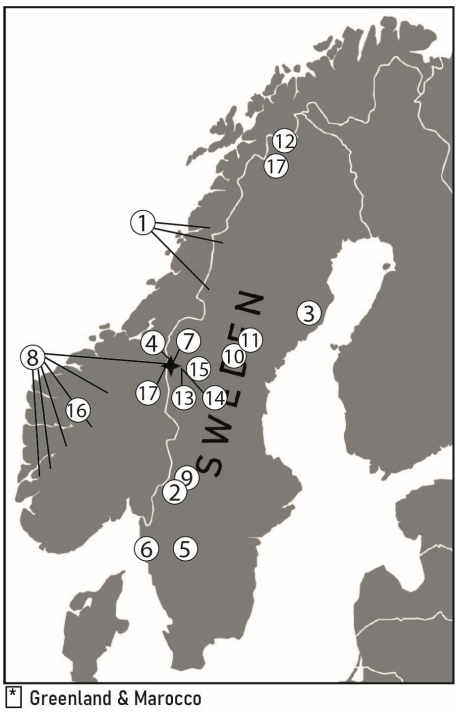

Figure 18. *continued.*

ciären, its LIA expansion was constrained only to the upper part of the valley and the glacier reached its maximum in about 1789, with other notable advances in around 1840, 1870 and 1890 AD. From that point, there was an overall retreat marked by extensive ridges deposited in the 1900s and 1930s. By the 1960s, Helagsglaciären had disintegrated into two units, only one of which was still actively eroding and dumping sediment on exposed overdeepened bedrock niche at the time of the fieldwork. However, even this active lobe has not produced a well-marked moraine ridge, indicating that the entire system has been in negative mass balance throughout the last decades, which is consistent with mass balance data for Helagsglaciären for 1999-2019 from World Glacier Monitoring Service (WGMS, 2021).

The little terrace with the smaller of the two proglacial lake plains is framed by a two-phased latero-frontal moraine R15/17. The ages span the 8th to 12th centuries AD which would be at the upper limit of the dating method and therefore should be regarded with caution. However, glaciers are known to have expanded in Scandinavia around that time (e.g. Rosqvist et al., 2004) and thus the ages of these landforms are regarded as at least broadly accurate. Similar results were observed at Austre Okstindbreen 300 km north of Helagsglaciären, where an advance around 1.3 ka was found to correspond to the Neoglacial maximum, while the LIA extent was smaller (Bakke et al., 2010).

The earlier Holocene sediments in the lower Helags valley and in the Handölan valley remain unconstrained. A radiocarbon date (11,237 – 10,939 yr cal. BP) produced by Kullman and Kjällgren (2000) is considered inaccurate as it would imply that pine trees were growing at the Helags valley under the waning Younger Dryas ice sheet (Stroeven et al., 2016), the margin of which was several 100s km to the south at that time, in a climate that would have required temperatures much warmer than found at similar altitudes today. Given these circumstances, this study attempts to narrow down the possible timing of the outermost deposits by means of comparison with other climatic and geomorphological records from Scandinavia.

5.3 Palaeoclimate reconstruction

Reconstructing paleoclimate can be challenging as, apart from historical sources, there are hardly any direct records of temperature, precipitation or wind strength and direction. Therefore one must resort to the use of environmental proxies that have been shown to be sensitive to the climatic parameters, bearing in mind that the signal they record might also respond to other factors or be dampened. Reconstruction of palaeoclimate from ELA is no different as rather than corresponding directly to mass balance at a specific time, a reconstructed ELA reflects longer-term averages of any given glacier's mass balance, provided it is in equilibrium (Rea, 2009). Moreover, the climatic parameters calculated in this study hold true only while assuming that the ELA-temperature-precipitation relationship described by Ohmura et al. (1992) does not change through time. Nevertheless, some additional insights about their validity can be gained from comparison with other independently reconstructed climatic proxies from Jämtland and Scandinavia.

Figure 18 presents a compilation of glacier fluctuations, temperature and wetness reconstructions through Holocene in Scandinavia to enable a comparison of reconstructed periods of Helagsglaciären's advances. Numerous sources from Scandinavia point to a severe climatic cooling and very wet conditions centred around the Finse event (8.2 ka). The scale of Helagsglaciären's early Holocene advance, inferred very cold and wet climate and considerable weathering of moraines R28-29 are strongly suggestive of deposition during the widespread in Jämtland 8.5-8 ka cooling and so this age is proposed here for this set of moraines.

The 8th to 12th centuries were a period of varying climate. Pronounced cooling was inferred around the 9/10th century (Rosqvist et al., 2004; Zhang et al., 2016) (Figure 18). This was followed by a well-defined MWP in the 10th to 12th centuries (Linderholm and Gunnarson, 2005; Zhang et al., 2016) during which the glaciers probably retreated. The climate was rather wet as inferred by Gunnarson et al. (2003) and reconstructed by Olsen et al. (2012) and Bakke et al. (2008), which all agree rather well with the climatic parameters calculated from Helagsglaciären's ELA around that time. Therefore, the interpreted age of R15/17 is narrowed here to span 9th-10th centuries AD.
It has been suggested that Scandinavia experienced a very variable climate during the LIA (Nesje et al., 2007; Rosqvist et al., 2013), with the coldest periods around the years 1600, 1750, 1770, 1840, 1870 and 1900 AD. Some of these coldest time periods have resulted in the production of distinct moraine sequences (e.g. Nesje et al., 2007; Bakke et al., 2010; Zhang et al., 2016). The summer temperatures deviated by

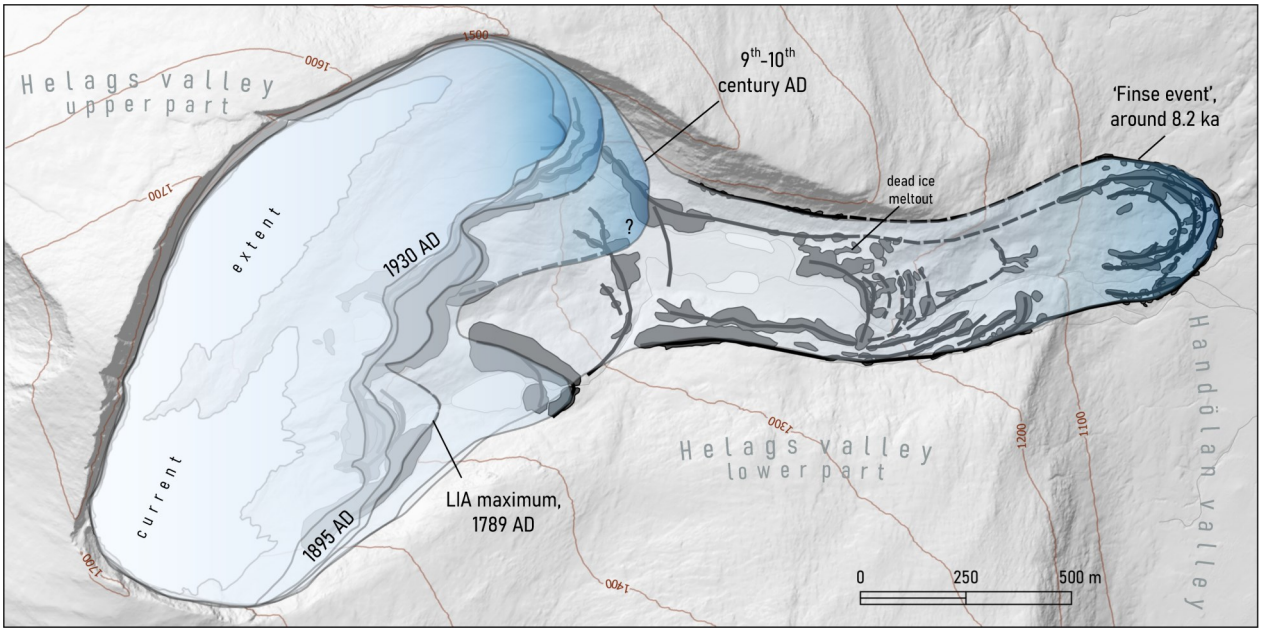

Figure 19. A synthesis figure showing the final interpretation of the chronology of retreat of Helagsglaciären. Grey polygons are mapped moraines from Figure 9. The thick black lines trace moraine crestlines. Dashed lines represent uncertain, inferred crestline trace.

about -1°C from the 1960-1990 mean (Zhang et al., 2016). This agrees very well with Helagsglaciären's periods of advance around 1790, 1840, 1870 and 1900 inferred from dated moraines R8, R10, R11, R13, R14 and R20 (Table 1).

Reconstructing palaeoprecipitation during the LIA is more problematic because wetness of an environment, apart from atmospheric factors, is heavily dependent on its hydrological regime which might be difficult to characterise in detail. This results in the lack of agreement between authors using proxies with different sensitivities to palaeoprecipitation.

According to Gunnarson et al. (2003) who derived his wetness reconstruction from Stömyren peat bog in south-central Sweden and a dendrochronological dataset, the time around 1790 AD experienced very wet conditions, which is in disagreement with the results in this study implying the period was the driest of all. However, other authors found weaker westerlies (Bakke et al., 2008) and a more negative North Atlantic Oscillation (NAO) index during the LIA (Olsen et al., 2012), both implying less humid conditions in western Scandinavia at this time which conforms to the climatic results from Helagsglaciären.

Bakke et al. (2008) used sediments from proglacial lakes fed by small glaciers with short response times along the coast of Norway, and calculated the said glaciers' ELAs. This proxy has a higher resolution than Gunnarson's et al. (2003) and is more similar to Helagsglaciären's palaeoprecipitation reconstruction methodology, so it is considered more relevant for comparison of precipitation. Olsen et al. (2012) used a lake sediment core from Greenland to reconstruct hypoxia and link it to lake water circulation changes indicative of changes in precipitation. Their reconstruction does not cover the 1790 AD, however, it agrees very well with Bakke et al. (2008) and shows a decrease in NAO strength at the beginning of the LIA.

Glueck and Stockton (2001) reconstructed NAO for period 1429-1983 AD using tree-ring chronologies from Morocco and Finland, and $\delta^{18}O$ and snow accumulation records from GISP2 ice core. Helagsglaciären's periods of advances fit into periods of both slightly negative and slightly positive NAO and thus remain being unequivocal. However, as Glueck and Stockton's (2001) chronology does not cover older periods reconstructed from Helagsglaciären, it is impossible to infer from it if the LIA was relatively drier or wetter than the other time periods.

All reviewed studies agree that the period from around the 8th to 12th centuries was wet or wetter than the LIA (Nesje et al., 2000; Gunnarson et al., 2003; Bakke et al., 2008; Andersson and Schoning, 2010; Andersson et al., 2010; Olsen et al., 2012; Rosqvist et al., 2013). Nesje et al. (2000) is the only study that addresses precipitation during the Finse event and also reconstructs very wet conditions at that time, similarly to the results from Helagsglaciären.

It is concluded that precipitation reconstruction from Helagsglaciären matches other records rather well, which is significant considering the glacier's small size and strong influence of topography on its dynamics.

5.4 Significance of Helagsglaciären for Holocene palaeoglacial reconstructions

To the author's knowledge, Helagsglaciären is the first glacier in Sweden for which a complete Holocene reconstruction has been attempted using both geomorphological mapping and ELA reconstruction, the results of which are summarised on Figure 19. Previous works on the topic either focused only on the LIA

(Regnéll and Hormes, 2015) or just the mapping (Karlén, 1973; Denton and Karlén, 1976). There is a limit to universal conclusions that can be derived from studying a single cirque or valley glacier. Nevertheless, several interesting points can be made from the research presented here.

Firstly, some present small cirque glaciers used to be more extensive, active glaciers in the past, which makes them possible analogues for the present, where glaciers are currently retreating rapidly due to global warming (e.g. Zemp et al., 2019). Investigating their dynamics and responses to climatic factors would prove to be useful in predicting the outcomes of current environmental change. Therefore, more effort should be put into unveiling the sedimentological and geomorphological record in the forelands of such glaciers and already-empty cirques.

Secondly, the dynamics of a medium-sized to small glacier can change through time due to combined effects of changes in climate and ice hypsometry, so that it is less or more responsive to the same climatic signal than those in the vicinity. A large influence on the timing of such a switch is possibly exerted by the overall size of the ice body (and especially thickness) which determines absolute mass loss or gain, but also response time at the snout (Bahr et al., 1998). Moreover, the southern location of Helagsglaciären probably determined its switch from polythermal to temperate regime, unlike current polythermal Arctic glaciers that are predicted to contain increasingly larger areas of cold bed (Glasser and Hambrey, 2001).

Thirdly, an extremely important factor in the dynamics of small valley/cirque glaciers is the local topography that determines the sensitivity of the snout. When included in regional palaeostudies, these glaciers should probably be reviewed on a case-by-case basis (cf. Kuhn et al., 1985).

Lastly, there is a wide-spread recognition that the behaviour of small cirque or valley glaciers may be heavily dependent on non-climatic factors like topography or snowblow and thus not conform to, or reflect general palaeoclimatic changes (Barr and Lovell, 2014). However, palaeoclimatic reconstruction at Helagsglaciären agrees well with other records from Scandinavia, though only a larger investigation involving a group of nearby glaciers would be able to ultimately confirm how reliable this study is. This warrants more attention to be paid to other similar glaciers in future palaeoclimatic studies.

6. Conclusions

This study attempted to reconstruct the glacier dynamics, chronology and palaeoclimate of Helagsglaciären throughout the Holocene by using geomorphological mapping, sedimentology, lichenometry and ELA calculation. A synthesis of conclusions is presented below.

1. The Helags valley sediments were mapped in detail and 21 moraines were dated by means of lichenometry (R4-R15, R17, R20-26 and R28) using a locally-derived calibration curve. Three sediment exposures were also dug in different moraines along the valley's length. The valley is occupied by extensive sediments of different ages much beyond the current extent of Helagsglaciären, indicating earlier prominent advances.

2. Based on the geomorphological and sedimentological evidence, Helagsglaciären switched from being a polythermal glacier in the past to the temperate one it is today. It disintegrated into two parts, one of which is still active despite its small size. That suggests a considerable thickness of the active part.

3. Topography plays a large role in the survival and behaviour of cirque and valley glaciers (including Helagsglaciären) and should be carefully considered when including them in palaeostudies.

4. Based on the comparison of palaeoclimatic data from Helagsglaciären and other studies from Scandinavia, it is suggested that Helagsglaciären reached a maximum probably around the Finse event (8.5-8.0 ka) when summer temperatures were almost as cold as during the LIA, but the climate was much wetter.

5. Other prominent advances were around the 9^{th}-10^{th} century AD, around 1790 (the LIA maximum) and 1900 AD, as inferred from lichenometry.

6. The LIA was the coldest and driest period out of the established chronology. Helagsglaciären did not reach its Neoglacial maximum at that time, but earlier around 9^{th}-10^{th} century.

7. The reconstructed glacier fluctuation chronology and calculated climatic data agree well with the local literature.

7. Acknowledgements

The author would like to thank Sven Lukas for great supervision and many insightful discussions throughout the course of designing, conducting and writing this thesis. Special thanks go to Oleg Zheleznyy for immeasurable help during the fieldwork and numerous brainstorms before and after it. I would also like to thank my examiners Helena Alexanderson and Mikael Calner. Many thanks to my family and friends for unwaning support regardless of what I do.

This work is dedicated to my geography teacher Mrs. Błoszyńska, who has always been with me.

7 References

Andersson, S., Rosqvist, G., leng, M. j., Wastegård, S., & Blaauw, M. (2010). Late holocene climate change in central Sweden inferred from Lacustrine stable isotope data. *Journal of Quaternary Science*, *25*(8), 1305–1316. https://doi.org/10.1002/jqs.1415

Andersson, S., & Schoning, K. (2010). Surface wetness and mire development during the late Holocene in central Sweden. *Boreas*, 39: 749-760. https://doi.org/10.1111/j.1502-3885.2010.00157.x

Antonsson, K., & Seppä, H. (2007). Holocene temperatures in Bohuslän, Southwest Sweden: A quantitative reconstruction from fossil pollen data. *Boreas*, *36*(4), 400–410. https://doi.org/10.1080/03009480701317421.

Armstrong, R. A. (2016). Lichenometric dating

(lichenometry) and the biology of the lichen genus Rhizocarpon: Challenges and future directions. *Geografiska Annaler: Series A, Physical Geography*, *98*(3), 183–206. https://doi.org/10.1111/geoa.12130

Bahr, D. B., Pfeffer, W. T., Sassolas, C., & Meier, M. F. (1998). Response time of glaciers as a function of size and mass balance: 1. theory. *Journal of Geophysical Research: Solid Earth*, *103*(B5), 9777–9782. https://doi.org/10.1029/98jb00507

Bakke, J., Dahl, S. O., Paasche, Ø., Riis Simonsen, J., Kvisvik, B., Bakke, K., & Nesje, A. (2010). A complete record of Holocene Glacier variability at Austre Okstindbreen, Northern Norway: An integrated approach. *Quaternary Science Reviews*, *29*(9–10), 1246–1262. https://doi.org/10.1016/j.quascirev.2010.02.012

Bakke, J., Lie, Ø., Dahl, S. O., Nesje, A., & Bjune, A. E. (2008). Strength and spatial patterns of the holocene wintertime westerlies in the NE atlantic region. *Global and Planetary Change*, *60*(1–2), 28–41. https://doi.org/10.1016/j.gloplacha.2006.07.030

Barr, I. D., & Lovell, H. (2014). A review of topographic controls on Moraine Distribution. *Geomorphology*, *226*, 44–64. https://doi.org/10.1016/j.geomorph.2014.07.030

Barnekow, L. (2000). Holocene regional and local vegetation history and lake-level changes in the Torneträsk area, northern Sweden. *Journal of Paleolimnology*, *23*(4), 399–420. https://doi.org/10.1023/a:1008171418429

Benedict, J. B. (2009). A review of lichenometric dating and its applications to archaeology. *American Antiquity*, *74*(1), 143–172. https://doi.org/10.1017/s0002731600047545

Benn, D. I., & Ballantyne, C. K. (2005). Palaeoclimatic reconstruction from Loch Lomond readvance glaciers in the West Drumochter Hills, Scotland. *Journal of Quaternary Science*, *20*(6), 577–592. https://doi.org/10.1002/jqs.925

Benn, D., & Evans, D. J. A. (2010). *Glaciers and Glaciation, 2nd edition*. Routledge. ISBN: 1444174002, 9781444174007.

Bergman, J. (2005). Tree-limit ecotonal response to Holocene climate change in the Scandes Mountains. PhD Thesis. Lund University, Department of Geology, Quaternary Sciences, LUNDQUA Thesis 53, 35 pp.

Bergman, J., Hammarlund, D., Hannon, G., Barnekow, L., & Wohlfarth, B. (2005). Deglacial vegetation succession and Holocene Tree-limit dynamics in the Scandes Mountains, west-central Sweden: Stratigraphic Data compared to megafossil evidence. *Review of Palaeobotany and Palynology*, *134*(3–4), 129–151. https://doi.org/10.1016/j.revpalbo.2004.12.005

Bergström, E. (1955). Studies of the variations in size of Swedish glaciers in recent centuries. *UGGI Ass. Int. d'Hydrologie. Publ*, *39*.

Beschel, R. (1955). Individuum und Alter bei Fletchten [Individuality and Age of Lichens]. *Phyton* 6:59-68.

Beschel, R. (1957). Lichenometrie im Gletschervorfeld [Lichenometry in the Glacier Foreland], *Jahrbuch zum Schutze der Alpenpflanzen und -Tiere* 22:164—185.

Beschel, R. (1958). Flechtenvereine der Stadte, Stadtflechten und ihr Wachstum [Lichen Associations in Cities, City Lichens, and Their Growth], *Berichte des Naturwissenschaftlich-Medizinischen Vereins in Innsbruck* 52:1-158

Björklund, J., Gunnarson, B. E., Seftigen, K., Zhang, P., & Linderholm, H. W. (2015). Using adjusted blue intensity data to attain high-quality summer temperature information: A case study from Central Scandinavia. *The Holocene*, *25*(3), 547–556. https://doi.org/10.1177/0959683614562434

Blomdin, R., Becher, G. P., Smith, C. A., Regnéll, C., Öhrling, C., Goodfellow, B. W. & Mikko, H. (2021). Beskrivning till geomorfologiska kartan Jämtlands län. Sveriges geologiska undersökning. ISBN 978-91-89421-12-7.

Bolin Centre for Climate Research. (2017). *Helagsglaciären*. Svenska glaciärer. https://bolin.su.se/data/svenskaglaciarer/glacier.php?g=62

Boston, C. M., & Lukas, S. (2019). Topographic controls on Plateau Icefield recession: Insights from the younger Dryas Monadhliath Icefield, Scotland. *Journal of Quaternary Science*, *34*(6), 433–451. https://doi.org/10.1002/jqs.3111

Boston, C. M., Lukas, S., & Carr, S. J. (2015). A younger Dryas plateau icefield in the Monadhliath, Scotland, and implications for regional palaeoclimate. *Quaternary Science Reviews*, *108*, 139–162. https://doi.org/10.1016/j.quascirev.2014.11.020.

Bradwell, T. (2009). Lichenometric Dating: A commentary, in the light of some recent statistical studies. *Geografiska Annaler: Series A, Physical Geography*, *91*(2), 61–69. https://doi.org/10.1111/j.1468-0459.2009.00354.x

Bradwell, T. (2010). Studies on the growth of Rhizocarpon Geographicum in NW Scotland, and some implications for lichenometry. *Geografiska Annaler: Series A, Physical Geography*, *92*(1), 41–52. https://doi.org/10.1111/j.1468-0459.2010.00376.x

Bradwell, T., & Armstrong, R. A. (2007). Growth rates ofrhizocarpon geographicum lichens: A review with new data from Iceland. *Journal of Quaternary Science*, *22*(4), 311–320. https://doi.org/10.1002/jqs.1058

Carr, S. J., Lukas, S., & Mills, S. C. (2010). Glacier Reconstruction and mass-balance modelling as a geomorphic and palaeoclimatic tool. *Earth Surface Processes and Landforms*, *35*(9), 1103–1115. https://doi.org/10.1002/esp.2034

Carrivick, J. L., & Brewer, T. R. (2004). Improving local estimations and regional trends of Glacier Equilibrium Line altitudes. *Geografiska Annaler: Series A, Physical Geography*, *86*(1), 67–79. https://doi.org/10.1111/j.0435-3676.2004.00214.x

Carturan, L., Baroni, C., Carton, A., Cazorzi, F., Fontana, G. D., Delpero, C., Salvatore, M. C., Seppi, R., & Zanoner, T. (2014). Reconstructing fluctuations of La Mare Glacier (eastern Italian Alps) in the late holocene: New evidence for a little ice age maximum around 1600 AD. *Geografiska Annaler: Series A, Physical Geography*, *96*(3), 287–306. https://doi.org/10.1111/geoa.12048

Chandler, B. M. P., Lovell, H., Boston, C. M., Lukas, S., Barr, I. D., Benediktsson, Í. Ö., Benn, D. I., Clark, C. D., Darvill, C. M., Evans, D. J. A., Ewertowski, M. W., Loibl, D., Margold, M., Otto, J.-C., Roberts, D. H., Stokes, C. R., Storrar, R. D., & Stroeven, A. P. (2018). Glacial geomorphological mapping: A review of approaches and frameworks for best practice. *Earth-Science Reviews*, *185*, 806–846. https://doi.org/10.1016/j.earscirev.2018.07.015

Chandler, B. M., & Lukas, S. (2017). Reconstruction of loch lomond stadial (younger Dryas) glaciers on Ben more Coigach, north-west Scotland, and implications for reconstructing palaeoclimate using small ice masses. *Journal of Quaternary Science*, *32*(4), 475–492. https://doi.org/10.1002/jqs.2941

Denton, G. H., & Karlén, W. (1973). Lichenometry: Its application to Holocene Moraine Studies in southern Alaska and Swedish Lapland. *Arctic and Alpine Research*, *5*(4), 347–372. https://doi.org/10.1080/00040851.1973.12003745

Digerfeldt, G. (1988). Reconstruction and regional correlation of Holocene Lake-level fluctuations in Lake Bysjön, South Sweden. *Boreas*, *17*(2), 165–182. https://doi.org/10.1111/j.1502-3885.1988.tb00544.x

Enquist, F. (1910). Über die jetzigen und ehemaligen lokalen Gletscher in den Gebirgen von Jämtland und Härjedalen.

Die Gletscher Schwedens im Jahre 1908. *Sveriges geologiska Undersökning,* Ca 5.V, 1–36.

Ericsson Rehn, I. (2019). Mass balance and local characteristics of three glaciers in southern Norway, between 1980 and 2018. An analysis of the mass balance and the local characteristics of Ålfotbreen, Storbreen and Gråsubreen. *Stockholm University Bachelor's thesis,* GG 242.

Evans, D. J. A. & Benn, D. (2021). Practical Guide to the Study of Glacial Sediments. 2nd edition. *Routledge*. ISBN: 9781138139206 .

Evans, D. J. A., Archer, S., & Wilson, D. J. H. (1999). A comparison of the lichenometric and Schmidt hammer dating techniques based on data from the proglacial areas of some Icelandic glaciers. *Quaternary Science Reviews*, *18*(1), 13–41. https://doi.org/10.1016/s0277-3791(98)00098-5

Faegri, K. (1934). Uber die Langenvariationen einiger Gletscher des Jostedalsbre und die dadurch bedingten Pflanzensukzessionen. *Bergens Museums Aarbog,* 1993: 137 –142.

Fries, C. (1931). Svenska Turistföreningens Årsskrift. Härjedalen.

Gjerde, M., Bakke, J., Vasskog, K., Nesje, A., & Hormes, A. (2016). Holocene glacier variability and neoglacial hydroclimate at ålfotbreen, Western Norway. *Quaternary Science Reviews*, *133*, 28–47. https://doi.org/10.1016/j.quascirev.2015.12.004

Glasser, N. F., & Hambrey, M. J. (2001). Styles of sedimentation beneath Svalbard valley glaciers under changing dynamic and thermal regimes. *Journal of the Geological Society*, *158*(4), 697–707. https://doi.org/10.1144/jgs.158.4.697

Glueck, M. F., & Stockton, C. W. (2001). Reconstruction of the North Atlantic Oscillation, 1429-1983. *International Journal of Climatology*, *21*(12), 1453–1465. https://doi.org/10.1002/joc.684

Greenwood, S. L., Clark, C. D., & Hughes, A. L. (2007). Formalising an inversion methodology for reconstructing ice-sheet retreat patterns from meltwater channels: Application to the British Ice Sheet. *Journal of Quaternary Science*, *22*(6), 637–645. https://doi.org/10.1002/jqs.1083

Gunnarson, B. E., Linderholm, H. W., & Moberg, A. (2010). Improving a tree-ring reconstruction from west-central Scandinavia: 900 years of warm-season temperatures. *Climate Dynamics*, *36*(1–2), 97–108. https://doi.org/10.1007/s00382-010-0783-5

Gunnarson, B. E., Borgmark, A., & Wastegård, S. (2003). Holocene humidity fluctuations in Sweden inferred from dendrochronology and peat stratigraphy. *Boreas*, *32*(2), 347–360. https://doi.org/10.1080/03009480310001641

Haakensen, N. (1989). Akkumulasjon på breene i Norge vinteren 1988–89. *Været*, *13*(91), e94.

Hammarlund, D., Velle, G., Wolfe, B. B., Edwards, T. W. D., Barnekow, L., Bergman, J., Holmgren, S., Lamme, S., Snowball, I., Wohlfarth, B., & Possnert, G. (2004). Palaeolimnological and sedimentary responses to holocene forest retreat in the Scandes Mountains, west-central Sweden. *The Holocene*, *14*(6), 862–876. https://doi.org/10.1191/0959683604hl756rp

Holmlund, P. & Jansson, P. (2003). Glaciologi. *Stockholm Universitet*. ISBN 9197454109.

Hughes, A. L. C., Clark, C. D., & Jordan, C. J. (2010). Subglacial Bedforms of the last British ice sheet. *Journal of Maps*, *6*(1), 543–563. https://doi.org/10.4113/jom.2010.1111

Humlum, O. (1978). Genesis of layered lateral moraines. *Geografisk Tidsskrift-Danish Journal of Geography*, *77* (1), 65–72. https://doi.org/10.1080/00167223.1978.10649094

Innes, J. L. (1983). Development of lichenometric dating curves for Highland Scotland. *Transactions of the Royal Society of Edinburgh: Earth Sciences*, *74*(1), 23–32. https://doi.org/10.1017/s0263593300009871

IPCC (2023). Summary for Policymakers. In: Climate Change 2023: Synthesis Report. A Report of the Intergovernmental Panel on Climate Change. Contribution of Working Groups I, II and III to the Sixth Assessment Report of the Intergovernmental Panel on Climate Change [Core Writing Team: H. Lee and J. Romero (eds.)]. IPCC, Geneva, Switzerland, 36 pages. (in press)

Irvine-Fynn, T. D., Hodson, A. J., Moorman, B. J., Vatne, G., & Hubbard, A. L. (2011). Polythermal Glacier Hydrology: A Review. *Reviews of Geophysics*, *49*(4), 2010RG000350. https://doi.org/10.1029/2010rg000350

Karlén, W. (1988). Scandinavian glacial and climatic fluctuations during the Holocene. *Quaternary Science Reviews*, *7*(2), 199–209. https://doi.org/10.1016/0277-3791(88)90006-6

Karlén, W. (1973). Holocene Glacier and climatic variations, Kebnekaise Mountains, Swedish Lapland. *Geografiska Annaler: Series A, Physical Geography*, *55*(1), 29–63. https://doi.org/10.1080/04353676.1973.11879879

Karlén, W., & Denton, G. H. (1976). Holocene glacial variations in Sarek National Park, northern Sweden. *Boreas*, *5*(1), 25–56. https://doi.org/10.1111/j.1502-3885.1976.tb00329.x

Kjær, K. H., & Kruger, J. (2001). The final phase of dead-ice moraine development: Processes and sediment architecture, Kötlujökull, Iceland. *Sedimentology*, *48*(5), 935–952. https://doi.org/10.1046/j.1365-3091.2001.00402.x

Kleman, J., & Stroeven, A. P. (1997). Preglacial surface remnants and quaternary glacial regimes in northwestern Sweden. *Geomorphology*, *19*(1–2), 35–54. https://doi.org/10.1016/s0169-555x(96)00046-3

Kleman, J., Hättestrand, C., Borgström, I., & Stroeven, A. (1997). Fennoscandian palaeoglaciology reconstructed using a glacial geological inversion model. *Journal of Glaciology*, *43*(144), 283–299. https://doi.org/10.1017/s0022143000003233

Krog-Larsen, N., Linge, H., Håkansson, L., & Fabel, D. (2012). Investigating the last deglaciation of the Scandinavian ice sheet in southwest Sweden with 10be exposure dating. *Journal of Quaternary Science*, *27*(2), 211–220. https://doi.org/10.1002/jqs.1536

Krog-Larsen, N., Knudsen, K. L., Krohn, C. F., Kronborg, C., Murray, A. S., & Nielsen, O. B. (2009). Late quaternary ice sheet, Lake and sea history of southwest Scandinavia - A synthesis. *Boreas*, *38*(4), 732–761. https://doi.org/10.1111/j.1502-3885.2009.00101.x

Krüger, J., & Kjær, K. H. (1999). A data chart for field description and genetic interpretation of glacial diamicts and associated sediments…with examples from Greenland, Iceland, and Denmark. *Boreas*, *28*(3), 386–402. https://doi.org/10.1111/j.1502-3885.1999.tb00228.x

Krüger, J., Kjær, K. H., & Van Der Meer, J. J. (2002). From push moraine to single-crested dump moraine during a sustained glacier advance. *Norsk Geografisk Tidsskrift - Norwegian Journal of Geography*, *56*(2), 87–95. https://doi.org/10.1080/002919502760056404

Kuhn, M., Markl, G., Kaser, G., Nickus, U., Obleitner, F., & Schneider, H. (1985). Fluctuations of climate and mass balance: different responses of two adjacent glaciers. *Zeitschrift für Gletscherkunde und Glazialgeologie*, *21* (1), 409-416.

Kullman, L., & Kjällgren, L. (2000). A coherent postglacial tree-limit chronology (Pinus sylvestris L.) for the Swedish scandes: Aspects of paleoclimate and "Recent warming," based on Megafossil Evidence. *Arctic, Antarctic,*

and Alpine Research, *32*(4), 419–428. https://doi.org/10.1080/15230430.2000.12003386
Lantmäteriet. (2022). *Geodataportalen*. Lantmateriet.se. https://www.lantmateriet.se/sv/geodata/Geodataportalen/
Larsson, T.B., Rosqvist, G., Ericsson, G. & Heinerud, J. (2012). Climate change, Mooses and Humans in Northern Sweden 4000 cal. yr. BP. *Journal of Northern Studies* 6, 9–30.
Leigh, J. R., Stokes, C. R., Evans, D. J., Carr, R. J., & Andreassen, L. M. (2020). Timing of Little Ice Age maxima and subsequent glacier retreat in Northern Troms and western Finnmark, Northern Norway. *Arctic, Antarctic, and Alpine Research*, *52*(1), 281–311. https://doi.org/10.1080/15230430.2020.1765520
Linderholm, H. W., & Gunnarson, B. E. (2005). Summer temperature variability in central Scandinavia during the last 3600 Years. *Geografiska Annaler: Series A, Physical Geography*, *87*(1), 231–241. https://doi.org/10.1111/j.0435-3676.2005.00255.x
Lipovsky, B. P., Meyer, C. R., Zoet, L. K., McCarthy, C., Hansen, D. D., Rempel, A. W., & Gimbert, F. (2019). Glacier sliding, seismicity and sediment entrainment. *Annals of Glaciology*, *60*(79), 182–192. https://doi.org/10.1017/aog.2019.24
Lukas, S. (2011). Ice-cored moraines. *Encyclopedia of snow, ice and glaciers*, 616-619.
Lukas, S., & Bradwell, T. (2010). Reconstruction of a late-glacial (Younger Dryas) mountain ice field in Sutherland, northwestern Scotland, and its palaeoclimatic implications. *Journal of Quaternary Science*, *25*(4), 567–580. https://doi.org/10.1002/jqs.1376
Lukas, S., Graf, A., Coray, S., & Schlüchter, C. (2012). Genesis, stability and preservation potential of large lateral moraines of alpine valley glaciers – towards a unifying theory based on findelengletscher, Switzerland. *Quaternary Science Reviews*, *38*, 27–48. https://doi.org/10.1016/j.quascirev.2012.01.022
Lundqvist, J. (1969). Beskrivning till Jordartskarta över Jämtlands län. *Sveriges geologiska undersökning*, Ca 45, 418 s.
Mallinson, L., Swift, D. A., & Sole, A. (2019). Proglacial icings as indicators of glacier thermal regime: Ice thickness changes and icing occurrence in Svalbard. *Geografiska Annaler: Series A, Physical Geography*, *101*(4), 334–349. https://doi.org/10.1080/04353676.2019.1670952
Matthews, J. A. (2005). 'Little Ice Age' glacier variations in Jotunheimen, southern Norway: A study in regionally controlled lichenometric dating of recessional moraines with implications for climate and lichen growth rates. *The Holocene*, *15*(1), 1–19. https://doi.org/10.1191/0959683605hl779rp
Mooers, H. D. (1990). A glacial-process model: The role of spatial and temporal variations in Glacier Thermal regime. *Geological Society of America Bulletin*, *102*(2), 243–251. https://doi.org/10.1130/0016-7606(1990)102<0243:agpmtr>2.3.co;2
Nesje, A., Dahl, S. O., Thun, T., & Nordli, Ø. (2007). The 'Little Ice Age' glacial expansion in western Scandinavia: Summer temperature or winter precipitation? *Climate Dynamics*, *30*(7–8), 789–801. https://doi.org/10.1007/s00382-007-0324-z
Nesje, A., Dahl, S. O., Thun, T., & Nordli, Ø. (2008). The 'Little Ice Age' glacial expansion in western Scandinavia: Summer temperature or winter precipitation? *Climate Dynamics*, *30*(7–8), 789–801. https://doi.org/10.1007/s00382-007-0324-z
Nesje, A., Lie, Ø., & Dahl, S. O. (2000). Is the North Atlantic oscillation reflected in Scandinavian glacier mass balance records? *Journal of Quaternary Science*, *15*(6), 587–601. https://doi.org/10.1002/1099-1417(200009)15:6<587::aid-jqs533>3.0.co;2-2
Nesje, A. (2009). Latest Pleistocene and Holocene Alpine Glacier fluctuations in Scandinavia. *Quaternary Science Reviews*, *28*(21–22), 2119–2136. https://doi.org/10.1016/j.quascirev.2008.12.016
Norris, S. L., Margold, M., & Froese, D. G. (2017). Glacial landforms of Northwest Saskatchewan. *Journal of Maps*, *13*(2), 600–607. https://doi.org/10.1080/17445647.2017.1342212
Ohmura, A., Kasser, P., & Funk, M. (1992). Climate at the equilibrium line of glaciers. *Journal of Glaciology*, *38*(130), 397–411. https://doi.org/10.3189/s0022143000002276
Olsen, J., Anderson, N. J., & Knudsen, M. F. (2012). Variability of the North Atlantic oscillation over the past 5,200 years. *Nature Geoscience*, *5*(11), 808–812. https://doi.org/10.1038/ngeo1589
OPENGIS.ch. (2022). *The most powerful and efficient way to manage your data on-the-go*. QField. https://qfield.org/
Osmaston, H. (2005). Estimates of glacier equilibrium line altitudes by the area×altitude, the area×altitude balance ratio and the area×altitude balance index methods and their validation. *Quaternary International*, *138–139*, 22–31. https://doi.org/10.1016/j.quaint.2005.02.004
Osmaston, H. A. (2006). Should quaternary sea-level changes be used to correct glacier ELAS, vegetation belt altitudes and sea level temperatures for inferring climate changes? *Quaternary Research*, *65*(02), 244–251. https://doi.org/10.1016/j.yqres.2005.11.004
O'Neal, M. A. (2006). The effects of slope degradation on lichenometric dating of Little Ice Age moraines. *Quaternary Geochronology*, *1*(2), 121–128. https://doi.org/10.1016/j.quageo.2006.05.025
Radić, V., & Hock, R. (2006). Modeling future glacier mass balance and volume changes using era-40 reanalysis and climate models: A sensitivity study at Storglaciären, Sweden. *Journal of Geophysical Research: Earth Surface*, *111*(F3). https://doi.org/10.1029/2005jf000440
Rasmussen, S. O., Andersen, K. K., Svensson, A. M., Steffensen, J. P., Vinther, B. M., Clausen, H. B., Siggaard-Andersen, M.-L., Johnsen, S. J., Larsen, L. B., Dahl-Jensen, D., Bigler, M., Röthlisberger, R., Fischer, H., Goto-Azuma, K., Hansson, M. E., & Ruth, U. (2006). A New Greenland Ice Core Chronology for the last glacial termination. *Journal of Geophysical Research*, *111*(D6). https://doi.org/10.1029/2005jd00607
Rea, B. R. (2009). Defining modern day area-altitude balance ratios (aabrs) and their use in glacier-climate reconstructions. *Quaternary Science Reviews*, *28*(3–4), 237–248. https://doi.org/10.1016/j.quascirev.2008.10.011
Regnéll, C., & Hormes, A. (2015). Holocene Equilibrium--Line Altitude (ELA) Reconstructions in Sarek National Park, Northern Sweden. In *45th International Arctic Workshop May 10–13, 2015*.
Reimer, P., Austin, W., Bard, E., Bayliss, A., Blackwell, P., Bronk Ramsey, C., . . . Talamo, S. (2020). The IntCal20 Northern Hemisphere Radiocarbon Age Calibration Curve (0–55 cal kBP). *Radiocarbon, 62*(4), 725-757. doi:10.1017/RDC.2020.41
Reinardy, B. T., Booth, A. D., Hughes, A. L., Boston, C. M., Åkesson, H., Bakke, J., Nesje, A., Giesen, R. H., & Pearce, D. M. (2019). Pervasive cold ice within a temperate glacier – implications for glacier thermal regimes, sediment transport and foreland geomorphology. *The Cryosphere*, *13*(3), 827–843. https://doi.org/10.5194/tc-13-827-2019
Reinardy, B. T., Leighton, I., & Marx, P. J. (2013). Glacier thermal regime linked to processes of annual moraine formation at Midtdalsbreen, Southern Norway. *Boreas*. https://doi.org/10.1111/bor.12008
Rettig, L., Lukas, S., & Huss, M. (2023). Implications of a rapidly thinning ice margin for annual Moraine Formation

at Gornergletscher, Switzerland. *Quaternary Science Reviews*, *308*, 108085. https://doi.org/10.1016/j.quascirev.2023.108085

Rosqvist, G. C., Leng, M. J., Goslar, T., Sloane, H. J., Bigler, C., Cunningham, L., Dadal, A., Bergman, J., Berntsson, A., Jonsson, C., & Wastegård, S. (2013). Shifts in precipitation during the last millennium in northern Scandinavia from Lacustrine Isotope Records. *Quaternary Science Reviews*, *66*, 22–34. https://doi.org/10.1016/j.quascirev.2012.10.030

Rosqvist, G., Jonsson, C., Yam, R., Karlén, W., & Shemesh, A. (2004). Diatom oxygen isotopes in pro-glacial lake sediments from northern Sweden: A 5000 year record of atmospheric circulation. *Quaternary Science Reviews*, *23*(7–8), 851–859. https://doi.org/10.1016/j.quascirev.2003.06.009

Seppä, H., Hammarlund, D., & Antonsson, K. (2005). Low-frequency and high-frequency changes in temperature and effective humidity during the Holocene in south-central Sweden: Implications for atmospheric and oceanic forcings of climate. *Climate Dynamics*, *25*(2–3), 285–297. https://doi.org/10.1007/s00382-005-0024-5

SGU (2021). *Jordarter 1:25 000 - 1:100 000*. Kartvisare. https://apps.sgu.se/kartvisare/kartvisare-jordarter-25-100.html

SGU (2017). *Berggrund geologi*. Kartvisare. https://apps.sgu.se/kartvisare/kartvisare-berg-50-250-tusen.html

SMHI (2013). *Nederbörd*. Svensk Meteorologisk och Hydrologisk Institutionen. https://www.smhi.se/kunskapsbanken/meteorologi/nederbord/nederbord-1.361

Snowball, I., Muscheler, R., Zillén, L., Sandgren, P., Stanton, T., & Ljung, K. (2010). Radiocarbon wiggle matching of Swedish lake varves reveals asynchronous climate changes around the 8.2 Kyr cold event. *Boreas*, *39*(4), 720–733. https://doi.org/10.1111/j.1502-3885.2010.00167.x

Snowball, I., Zillén, L., & Gaillard, M.-J. (2002). Rapid early-holocene environmental changes in northern Sweden based on studies of two varved lake-sediment sequences. *The Holocene*, *12*(1), 7–16. https://doi.org/10.1191/0959683602hl515rp

Snowball, I., & Sandgren, P. (1996). Lake sediment studies of holocene glacial activity in the Kårsa Valley, northern Sweden: Contrasts in interpretation. *The Holocene*, *6*(3), 367–372. https://doi.org/10.1177/095968369600600312

Stroeven, A. P., Hättestrand, C., Kleman, J., Heyman, J., Fabel, D., Fredin, O., Goodfellow, B. W., Harbor, J. M., Jansen, J. D., Olsen, L., Caffee, M. W., Fink, D., Lundqvist, J., Rosqvist, G. C., Strömberg, B., & Jansson, K. N. (2016). Deglaciation of Fennoscandia. *Quaternary Science Reviews*, *147*, 91–121. https://doi.org/10.1016/j.quascirev.2015.09.016

Sundqvist, H. S., Holmgren, K., & Lauritzen, S.-E. (2007). Stable isotope variations in stalagmites from northwestern Sweden document climate and environmental changes during the early holocene. *The Holocene*, *17*(2), 259–267. https://doi.org/10.1177/0959683607073292

Svendsen, J. I., Alexanderson, H., Astakhov, V. I., Demidov, I., Dowdeswell, J. A., Funder, S., Gataullin, V., Henriksen, M., Hjort, C., Houmark-Nielsen, M., Hubberten, H. W., Ingólfsson, Ó., Jakobsson, M., Kjær, K. H., Larsen, E., Lokrantz, H., Lunkka, J. P., Lysså, A., Mangerud, J., … Stein, R. (2004). Late quaternary ice sheet history of Northern Eurasia. *Quaternary Science Reviews*, *23*(11–13), 1229–1271. https://doi.org/10.1016/j.quascirev.2003.12.008

Syverson, K. M., & Mickelson, D. M. (2009). Origin and significance of lateral meltwater channels formed along a temperate glacier margin, Glacier Bay, Alaska. *Boreas*, *38*(1), 132–145. https://doi.org/10.1111/j.1502-3885.2008.00042.x

Tonkin, T. N., Midgley, N. G., Graham, D. J., & Labadz, J. C. (2016). Internal structure and significance of ice-marginal moraine in the Kebnekaise Mountains, northern Sweden. *Boreas*, *46*(2), 199–211. https://doi.org/10.1111/bor.12220

Velle, G., Brooks, S. J., Birks, H. J. B., & Willassen, E. (2005). Chironomids as a tool for inferring holocene climate: An assessment based on six sites in southern Scandinavia. *Quaternary Science Reviews*, *24*(12–13), 1429–1462. https://doi.org/10.1016/j.quascirev.2004.10.010

Wastegård, S. (2022). The holocene of sweden – A Review. *GFF*, *144*(2), 126–149. https://doi.org/10.1080/11035897.2022.2086290

Winkler, S. (2004). Lichenometric dating of the 'Little Ice Age' maximum in Mt Cook National Park, Southern Alps, New Zealand. *The Holocene*, *14*(6), 911–920. https://doi.org/10.1191/0959683604hl767rp

WGMS (2021). *Data exploration*. World Glacier Monitoring Service. https://wgms.ch/data-exploration/

Wyshnytzky, C. E., Lukas, S., & Groves, J. W. E. (2021). Multiple mechanisms of minor moraine formation in the Schwarzensteinkees Foreland, Austria. *Untangling the Quaternary Period—A Legacy of Stephen C. Porter*. https://doi.org/10.1130/2020.2548(10)

Zemp, M., Huss, M., Thibert, E., Eckert, N., McNabb, R., Huber, J., Barandun, M., Machguth, H., Nussbaumer, S. U., Gärtner-Roer, I., Thomson, L., Paul, F., Maussion, F., Kutuzov, S., & Cogley, J. G. (2019). Global Glacier Mass changes and their contributions to sea-level rise from 1961 to 2016. *Nature*, *568*(7752), 382–386. https://doi.org/10.1038/s41586-019-1071-0

Zhang, P., Linderholm, H. W., Gunnarson, B. E., Björklund, J., & Chen, D. (2016). 1200 years of warm-season temperature variability in central Scandinavia inferred from tree-ring density. *Climate of the Past*, *12*(6), 1297–1312. https://doi.org/10.5194/cp-12-1297-2016

Öberg, L., & Kullman, L. (2011). Recent glacier recession - a new source of postglacial treeline and climate history in the Swedish scandes. *Landscape Online*, *26*, 1–38. https://doi.org/10.3097/lo.201126

Appendix

Python script to calculate Equilibrium Line Altitude from a DEM of a glacier's surface using the AAR and AABR methods:

```
## import necessary libraries
import rasterio as rio
import numpy as np

# Define the input parameters
interval= 10
br= 1.9
cellsize=2

#### in order to import your dem raster, you use rasterio.
# Define relative path to file
dem_pre_path = "C:/Users/jelon/Desktop/Master_thesis/GIS data/Ice contours/iceDEMs/ice_DEM123.tif"

# Open the file using a context manager ("with rio.open" statement)
with rio.open(dem_pre_path) as dem_src:
dem = dem_src.read(1)                              #now you should have a numpy array of your ice DEM

# Maximum and minimum value of DEM
maxalt=dem.max()
print("Maximum ice elevation: ",maxalt)
dem[dem==-99999.0]=np.nan                          #set nans to all zeros
dem=dem[~np.isnan(dem)]                            #remove all nans, transform it to 1D array
minalt=dem.min()
print("Minimum ice elevation: ",minalt)

# create an empty list
# calculate ELA using AA method
for ela in np.arange(minalt,maxalt,1):             #take every possible ELA of the glacier in 1m steps
  list=[]
  for i in np.arange(minalt,maxalt,interval):      #for each contour belt of interval set above,
   area=dem[(i<dem) & (dem<(i+interval))].size*cellsize**2 #take the number of pixels within it and
                                                   #multiply by pixel area to get contour belt area
   ave_alt_diff=(i+(i+interval))/2-ela             #compute the difference between the contour average
                                                   #altitude and the ELA. If above the ELA, it's (+,
                                                   #accumulation), below its's (-, ablation)
   multiplication=area*ave_alt_diff                #weight the contour belt areas by their distance to ELA
   list.append(multiplication)                     #pool your results for each contour belt in the empty list
  suma=np.sum(list)                                #sum it all up
  if (suma<0):                                     #the first sum that becomes negative (change of
                                                   #sign, around zero), is printed
   print("AA method ELA is:", ela)                 #the ELA is calculated with the resolution of 1 m
   break

# create an empty list
# calculate ELA using AABR method
for ela in np.arange(minalt,maxalt,1):             #take every possible ELA of the glacier in 1m steps
  list=[]                                          #if the contour belt is below ELA...
  for i in np.arange(minalt,maxalt,interval):
   area=dem[(i<dem) & (dem<(i+interval))].size*cellsize**2
   ave_alt_diff=(i+(i+interval))/2-ela
   if ave_alt_diff<0:
     ave_alt_diff=ave_alt_diff*br                  #...you multiply it by Balance Ratio set above
   multiplication=area*ave_alt_diff
   list.append(multiplication)
  suma=np.sum(list)
  if (suma<0):
   print("AABR method ELA is:", ela)
   break
```

Tidigare skrifter i serien ”Examensarbeten i Geologi vid Lunds universitet”:

606. Tan, Brian, 2020: Nordvästra Skånes prekambriska geologiska utveckling. (15 hp)
607. Taxopoulou, Maria Eleni, 2020: Metamorphic micro-textures and mineral assemblages in orthogneisses in NW Skåne – how do they correlate with technical properties? (45 hp)
608. Damber, Maja, 2020: A palaeoecological study of the establishment of beech forest in Söderåsen National Park, southern Sweden. (45 hp)
609. Karastergios, Stylianos, 2020: Characterization of mineral parageneses and metamorphic textures in eclogite- to high-pressure granulite-facies marble at Allmenningen, Roan, western Norway. (45 hp)
610. Lindberg Skutsjö, Love, 2021: Geologiska och hydrogeologiska tolkningar av SkyTEM-data från Vombsänkan, Sjöbo kommun, Skåne. (15 hp)
611. Hertzman, Hanna, 2021: Odensjön - A new varved lake sediment record from southern Sweden. (45 hp)
612. Molin, Emmy, 2021: Rare terrestrial vertebrate remains from the Pliensbachian (Lower Jurassic) Hasle Formation on the Island of Bornholm, Denmark. (45 hp)
613. Höjbert, Karl, 2021: Dendrokronologi — en nyckelmetod för att förstå klimat- och miljöförändringar i Jämtland under holocen. (15 hp)
614. Lundgren Sassner, Lykke, 2021: A Method for Evaluating and Mapping Terrestrial Deposition and Preservation Potential for Palaeostorm Surge Traces. Remote Mapping of the Coast of Scania, Blekinge and Halland, in Southern Sweden, with a Field Study at Dalköpinge Ängar, Trelleborg. (45 hp)
615. Granbom, Johanna, 2021: En detaljerad undersökning av den mellanordoviciska ”furudalkalkstenen” i Dalarna. (15 hp)
616. Greiff, Johannes, 2021: Oolites from the Arabian platform: Archives for the aftermath of the end-Triassic mass extinction. (45 hp)
617. Ekström, Christian, 2021: Rödfärgade utfällningar i dammanläggningar orsakade av G. ferruginea och L. ochracea— Problemstatistik och mikrobiella levnadsförutsättningar. (15 hp)
618. Östsjö, Martina, 2021: Geologins betydelse i samhället och ett första steg mot en geopark på Gotland. (15 hp)
619. Westberg, Märta, 2021: The preservation of cells in biomineralized vertebrate tissues of Mesozoic age – examples from a Cretaceous mosasaur (Reptilia, Mosasauridae). (45 hp)
620. Gleisner, Lovisa, 2021: En detaljerad undersökning av kalkstenslager i den mellanordoviciska gullhögenformationen på Billingen i Västergötland. (15 hp)
621. Bonnevier Wallstedt, Ida, 2021: Origin and early evolution of isopods - exploring morphology, ecology and systematics. (15 hp)
622. Selezeneva, Natalia, 2021: Indications for solar storms during the Last Glacial Maximum in the NGRIP ice core. (45 hp)
623. Bakker, Aron, 2021: Geological characterisation of geophysical lineaments as part of the expanded site descriptive model around the planned repository site for high-level nuclear waste, Forsmark, Sweden. (45 hp)
624. Sundberg, Oskar, 2021: Jordlagerföljden i Höjeådalen utifrån nya borrningar. (15 hp)
625. Sartell, Anna, 2021: The igneous complex of Ekmanfjorden, Svalbard: an integrated field, petrological and geochemical study. (45 hp)
626. Juliusson, Oscar, 2021: Implications of ice-bedrock dynamics at Ullstorp, Scania, southern Sweden. (45 hp)
627. Eng, Simon, 2021: Rödslam i svenska kraftdammar - Problematik och potentiella lösningar. (15 hp)
628. Kervall, Hanna, 2021: Feasibility of Enhanced Geothermal Systems in the Precambrian crystalline basement in SW Scania, Sweden. (45 hp)
629. Smith, Thomas, 2022: Assessing the relationship between hypoxia and life on Earth, and implications for the search for habitable exoplanets. (45 hp)
630. Neumann, Daniel, 2022: En mosasaurie (Reptilia, Mosasauridae) av paleocensk ålder? (15 hp)
631. Svensson, David, 2022: Geofysisk och geologisk tolkning av kritskollors utbredning i Ystadsområdet. (15 hp)
632. Allison, Edward, 2022: Avsättning av Black Carbon i sediment från Odensjön, södra Sverige. (15 hp)
633. Jirdén, Elin, 2022: OSL dating of the Mesolithic site Nilsvikdalen 7, Bjorøy, Norway. (45 hp)
634. Wong, Danny, 2022: GIS-analys av effekten vid stormflod/havsnivåhöjning, Morupstrakten, Halland. (15 hp)
635. Lycke, Björn, 2022: Mikroplast i vattenavsatta sediment. (15 hp)
636. Schönherr, Lara, 2022: Grön fältspat i Varbergskomplexet. (15 hp)
637. Funck, Pontus, 2022: Granens ankomst och etablering i Skandinavien under postglacial tid. (15 hp)
638. Brotzen, Olga M., 2022: Geologiska besöksmål

och geoparker som plattform för popularisering av geovetenskap. (15 hp)

639. Lodi, Giulia, 2022: A study of carbon, nitrogen, and biogenic silica concentrations in Cyperus papyrus, the sedge dominating the permanent swamp of the Okavango Delta, Botswana, Africa. (45 hp)
640. Nilsson, Sebastian, 2022: PFAS- En sammanfattning av ny forskning, med ett fokus på föroreningskällor, provtagning, analysmetoder och saneringsmetoder. (15 hp)
641. Jägfeldt, Hans, 2022: Molnens påverkan på jordens strålningsbalans och klimatsystem. (15 hp)
642. Sundberg, Melissa, 2022: Paleontologiska egenskaper och syreisotopsutveckling i borrkärnan Limhamn-2018: Kopplingar till klimatförändringar under yngre krita. (15 hp)
643. Bjermo, Tim, 2022: A re-investigation of hummocky moraine formed from ice sheet decay using geomorphological and sedimentological evidence in the Vomb area, southern Sweden. (45 hp)
644. Halvarsson, Ellinor, 2022: Structural investigation of ductile deformations across the Frontal Wedge south of Lake Vättern, southern Sweden. (45 hp)
645. Brakebusch, Linus, 2022: Record of the end-Triassic mass extinction in shallow marine carbonates: the Lorüns section (Austria). (45 hp)
646. Wahlquist, Per, 2023: Stratigraphy and palaeoenvironment of the early Jurassic volcaniclastic strata at Djupadalsmölla, central Skåne, Sweden. (45 hp)
647. Gebremedhin, G. Gebreselassie, 2023: U-Pb geochronology of brittle deformation using LA-ICP-MS imaging on calcite veins. (45 hp)
648. Mroczek, Robert, 2023: Petrography of impactites from the Dellen impact structure, Sweden. (45 hp)
649. Gunnarsson, Niklas, 2023: Upper Ordovician stratigraphy of the Stora Sutarve core (Gotland, Sweden) and an assessment of the Hirnantian Isotope Carbon Excursion (HICE) in high-resolution. (45 hp)
650. Cordes, Beatrix, 2023: Vilken ny kunskap ger aDNA-analyser om vegetationsutvecklingen i Nordeuropa under och efter Weichsel-istiden? (15 hp)
651. Bonnevier Wallstedt, Ida, 2023: Palaeocolour, skin anatomy and taphonomy of a soft-tissue ichthyosaur (Reptilia, Ichthyopterygia) from the Toarcian (Lower Jurassic) of Luxembourg. (45 hp)
652. Kryffin, Isidora, 2023: Exceptionally preserved fish eyes from the Eocene Fur Formation of Denmark – implications for palaeobiology, palaeoecology and taphonomy. (45 hp)
653. Andersson, Jacob, 2023: Nedslagskratrars inverkan på Mars yt-datering. En undersökning av Mars främsta ytdateringsmetod ”Crater Counting". (15 hp)
654. Sundberg, Melissa, 2023: A study in ink – the morphology, taphonomy and phylogeny of squid -like cephalopods from the Jurassic Posidonia Shale of Germany and the first record of a loligosepiid gill. (45 hp)
655. Häggblom, Joanna, 2023: En patologisk sjölilja från silur på Gotland, Sverige. (15 hp)
656. Bergström, Tim, 2023: Hur gammal är jordens inre kärna? (15 hp)
657. Bollmark, Viveka, 2023: Ca isotope, oceanic anoxic events and the calcareous nannoplankton. (15 hp)
658. Madsen, Ariella, 2023: Polycykliska aromatiska kolväten i Hanöbuktens kustnära sediment - En sedimentologisk undersökning av vikar i närhet av pappersbruk. (15 hp)
659. Wangritthikraikul, Kannika, 2023: Holocene Environmental History of Warming Land, Northern Greenland: a study based on lake sediments. (45 hp)
660. Kurop, Anna, 2023: Reconstruction of the glacier dynamics and Holocene chronology of retreat of Helagsglaciären in Central Sweden. (45 hp)

LUNDS UNIVERSITET

Geologiska institutionen
Lunds universitet
Sölvegatan 12, 223 62 Lund